*Int. J. Solids Structures* Vol. 30, No. 19, pp. 2611–2638, 1993
Printed in Great Britain

0020–7683/93 $6.00+.00


# REFINED SHEAR-DEFORMATION MODELS FOR COMPOSITE LAMINATES WITH FINITE ROTATIONS

YAVUZ BAŞAR, YUNHE DING and REINHILD SCHULTZ
Ruhr-Universität Bochum, Bauingenieurwesen, Statik und Dynamik,
Universitatsstrasse 150, 4630 Bochum, Germany

(*Received* 2 *November* 1992; *in revised form* 23 *February* 1993)

**Abstract**—For arbitrary multilayered shell structures made particularly of composite material layers a refined finite-rotation theory with seven independent displacement variables is developed, approximating the displacement field by a cubic series expansion of thickness coordinates. This model allows a quadratic shear deformation distribution across the thickness. Procedures are given permitting a unique determination of the first order displacement term in the case of finite rotations. Kinematic relations are formulated in two alternative forms suitable for both classical and isoparametric finite element formulations. The constitutive relations presented model orthotropic material properties varying arbitrarily across the thickness. This third order single-layer theory is then transformed, by introducing further constraints, into three simplified models: a third order theory with five independent displacement variables, a Mindlin–Reissner type theory and a Kirchhoff–Love type theory. These four models differ, however, from each other essentially in the constraints imposed on the first and third order displacement variables: a significant advantage for a unified finite element development. Finally, the Mindlin–Reissner type theory is generalized to a layer-wise model being the most predictive one in dealing with local interlaminar effects. The theoretical models are transformed into adequate finite shell elements and then compared by means of appropriate examples concerning their prediction capability. Also examples are given demonstrating their applicability to finite-rotation phenomena.

## 1. INTRODUCTION

Because of a number of beneficial properties composite laminates have been becoming increasingly important in various branches of modern technology. When composite laminates are used in structural design, an essential objective is mostly to minimize the weight. Such a purpose evidently requires a special care in developing analysis models for this structure class. Now, the question is how can the analysis accuracy of the classical analysis models existing for isotropic shell structures be improved?

An essential decision to be made in developing refined analysis models for composite laminates concerns primarily the adoption of a kinematic model being more predictive in the calculation of transverse shear strains than those used in classical shell models (*theories of Kirchhoff–Love and Mindlin–Reissner type*). Comparative studies performed by many authors [e.g. Seide and Chaudhuri (1987), Pandya and Kant (1988), Reddy *et al.* (1989), and Başar *et al.* (1992b)] have clearly demonstrated that the classical shell models even of Mindlin–Reissner type are not able to predict the deformation behaviour with sufficient accuracy if the side length–thickness ratio or layer stiffness discontinuities exceed certain limits. Kinematic concepts proposed in the literature [see, e.g. Reddy (1989) and Reddy *et al.* (1989)] to improve the analysis accuracy in such situations are essentially of two different types. The first one consists of the approximation of the displacement field by a higher order series expansion (mainly a cubic one), leading to the so-called *higher order (refined) single-layer theories*. Thereby, *single-layer* theories are, according to the classification of Reddy (1989), to be understood as formulations where the displacement field possesses at least a $C^1$-continuity across the thickness and which therefore cover the above-mentioned classical shell models as special cases. The second concept being the basis of the so-called *layer-wise theories* is characterized by the fact that the given structure is first subdivided into a suitable number of sub-elements and each of them is then described by a Mindlin–Reissner type theory, imposing on the displacement field a $C^0$-continuity on all interfaces. This leads by a selection of $N$ sub-elements to a theoretical model with $2N+3$ independent displacements. Models of this type are, of course, the most expensive ones, but provide

results in every desired order of accuracy by a suitable sub-division. In the following both the models, the third order single-layer theory and the layer-wise theory, will be referred to as *refined models*.

The first shear-deformation model was proposed by Reissner (1945) for the linear plate analysis. This kinematic model and the Kirchhoff–Love hypothesis have governed during many decades the shell theory formulations [see, e.g. Başar and Krätzig (1985)] until certain inadequacies became apparent in modelling multilayered shell structures. This has motivated in recent time large research activities with the aim being to achieve more accurate analysis models for shells. The first third-order plate theories were proposed by Lo *et al.* (1977) and Reddy (1984). In Reddy's (1984) model presented for linear analysis, zero shear strain conditions on plate faces have been used leading to a formulation which possesses the same number of independent displacements as the Mindlin–Reissner type plate theory. This kinematic model and similar ones have then received a widespread use in modelling multilayered structures for different purposes, i.e. bending, stability and dynamic analysis [see, e.g. Phan and Reddy (1985), Kwon and Akin (1987), Bicos and Springer (1989), Cederbaum and Librescu (1989), Doxsee (1989), Reddy (1989), Shalev and Aboudi (1991), and Palazotto and Linnemann (1991)]. In many of the works cited above the attention is focused *a priori* on special shell geometries, mainly plates. Nonlinearities in connection with third-order kinematic models are considered in literature rarely and moreover by a restricted manner [e.g. Reddy (1989)]. The aspects cited above present strong limitations for applications in the field of composite laminates and show the necessity to extend the third-order kinematic model to new applications.

Comparatively refined models of layer-wise type have received less attention in the first development phase. The various layer-wise theories published in the literature differ from each other in the inclusion of transverse normal stresses and the degree of nonlinearities considered. Finite element formulations assuming transverse inextensibility are given by Owen and Li (1987a, b), Seide and Chaudhuri (1987), Reddy (1989), Reddy *et al.* (1989), and Rammerstorfer (1991). Formulations including transverse normal deformations are described by Epstein and Glockner (1977), and Epstein and Huttelmeier (1983). Most of the works cited above are not able to deal with finite rotations.

For the numerical analysis of composite laminates on the basis of classical kinematic models we refer to the contributions of Dorninger (1989), Dorninger and Rammerstorfer (1990), Eschenauer and Fuchs (1987), and Klarmann (1991). Nonlinearities are considered by Klarmann as finite rotations while, in contrast to recent tendencies in the nonlinear field, the moderate rotation concept has been adopted in Palmerio *et al.* (1990a, b) for the consideration of nonlinearities. For comprehensive reviews of refined models for the analysis of composite laminates we refer to Reddy (1989) and Noor *et al.* (1991).

Composite laminates used in modern technology are mostly very flexible structures. Accordingly, the consideration of nonlinearities with the accompanied instability phenomena is of great relevance for the design. This, in turn, may be achieved in a reliable form if finite rotations are *a priori* involved in the analysis. As can clearly be deduced from many comparative studies [see, e.g. Stein *et al.* (1982), Nolte (1983), Başar and Ding (1990) and Ding (1989)] simplified nonlinear models even of moderate rotation type may introduce significant errors in the analysis and are, moreover, not necessarily much more time-saving than finite-rotation models. Conclusively one may say that the moderate rotation concept presents for today's computational mechanics no advantages [see, e.g. Başar (1987)]. Finite-rotation models are the single models permitting a reliable nonlinear structural analysis in the whole nonlinear range. For the finite-rotation analysis of isotropic shells on the basis of classical hypotheses there exist already a large number of theoretical models [see, e.g. Pietraszkiewicz (1984, 1989), Stein *et al.* (1984), Simo and Fox (1989), Başar (1987) and Başar and Krätzig (1990) and references presented in these works] which have also been transformed in recent time into efficient finite elements (Recke and Wunderlich, 1986; Gruttmann *et al.*, 1989; Simo *et al.*, 1990; Büchter, 1992; Büchter and Ramm, 1992; Sansour and Bufler, 1992; Ding, 1989; Başar and Ding, 1990; Başar *et al.*, 1992a). But analysis models applicable to arbitrary multilayered shell structures where higher-order kinematic models and finite-rotations are considered in combination still seem to be lacking

in the literature. This has motivated the present contribution; its main objectives can be summarized as follows: A unified derivation of various shear-deformation models with the ability to deal with finite-rotations, the transformation of these models into finite shell elements and a comparative numerical study showing the prediction capability of the different analysis models, this last aspect being of particular interest to discover where and why refined analysis models are needed.

The starting point of the derivation of all theoretical models is the refined theory with a third-order displacement approximation. Since, unlike in some earlier formulations [e.g. Reddy (1989)], the vanishing of transverse shear strains on laminate faces is not explicitly required this model involves seven independent displacements. The constraint in question has been shown to be numerically inconvenient as it involves the second partial derivatives of the first order displacement term. Concerning the finite element implementation the distinction between refined models with five and seven independent variables is similar to that of classical models of Kirchhoff–Love and Mindlin–Reissner type.

The finite element formulation is accomplished using essentially the concepts of earlier developments (Ding, 1989; Başar and Ding, 1990; Başar *et al.*, 1992a) which have been shown to be numerically efficient. This concerns particularly the consideration of finite-rotations. Thus, for an *a priori* satisfaction of the unit length condition $\mathbf{a}_3 \cdot \mathbf{a}_3 = 1$ the deformed normal vector $\mathbf{a}_3$ is transformed into Euler rotation angles (Ramm, 1976) which are then, in contrast to the degeneration approach, directly interpolated in the finite element implementation.

## 2. GEOMETRY OF THE UNDEFORMED LAMINATE

In this paper, shell equations are presented in tensor formulation. As usual, Greek indices represent the numbers 1, 2 and Latin ones the numbers 1, 2, 3. We first consider the undeformed state of an arbitrary laminate (Fig. 1). Let $\mathring{\mathbf{r}} = \mathring{\mathbf{r}}(\theta^\alpha)$ be the position vector of a point $\mathring{P}$ of the undeformed middle surface $\mathring{F}$ where $\theta^\alpha$ are arbitrary curvilinear coordinates. Similar to $\mathring{\mathbf{r}}$, all geometrical elements associated with the undeformed state will be denoted by the suffix$(.\mathring{.})$. Thus, variables describing the undeformed middle surface geometry can be presented as:

$$\text{base vectors: } \mathring{\mathbf{a}}_\alpha = \mathring{\mathbf{r}}_{,\alpha} = \mathring{X}^i_{,\alpha}\mathbf{i}_i, \tag{1}$$

$$\text{metric tensor, determinant: } \mathring{a}_{\alpha\beta} = \mathring{\mathbf{a}}_\alpha \cdot \mathring{\mathbf{a}}_\beta,\ \mathring{a} = |\mathring{a}_{\alpha\beta}|, \tag{2}$$

$$\text{unit normal vector: } \mathring{\mathbf{n}}_3 = \mathring{\mathbf{a}}_3, \tag{3}$$

$$\text{curvature tensor: } \mathring{b}_{\alpha\beta} = -\mathring{\mathbf{a}}_\alpha \cdot \mathring{\mathbf{n}}_{3,\beta} = -\mathring{\mathbf{a}}_\alpha \cdot \mathring{\mathbf{a}}_{3,\beta}. \tag{4}$$

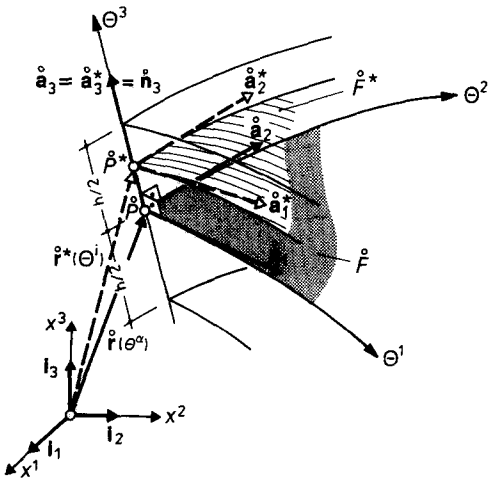


Fig. 1. Geometry of the undeformed shell continuum.

Partial derivatives with respect to $\theta^\alpha$ will be denoted by $(\ldots)_{,\alpha}$ and covariant derivatives with respect to the middle surface $\mathring{F}$ by $(\ldots)|_\alpha$.

Let $\theta^3$ be the distance of an arbitrary laminate point $\mathring{P}^*$, measured in the $\mathring{\mathbf{n}}_3$-direction. Thus, from the position vector of $\mathring{P}^*$

$$\mathring{\mathbf{r}}^* = \mathring{\mathbf{r}} + \theta^3 \mathring{\mathbf{a}}_3 \tag{5}$$

we find for the base vectors related to $\mathring{P}^*$:

$$\mathring{\mathbf{a}}_\alpha^* = \mathring{\mathbf{r}}_{,\alpha}^* = \mathring{\mathbf{r}}_{,\alpha} + \theta^3 \mathring{\mathbf{a}}_{3,\alpha} = \mathring{\mu}_\alpha^\rho \mathring{\mathbf{a}}_\rho, \quad \mathring{\mu}_\alpha^\rho = \delta_\alpha^\rho - \theta^3 \mathring{b}_\alpha^\rho, \tag{6}$$

$$\mathring{\mathbf{a}}_3^* = \mathring{\mathbf{n}}_3 = \mathring{\mathbf{a}}_3. \tag{7}$$

Herein, the notation $(\ldots)^*$ characterizes variables associated with the laminate continuum $\mathring{P}^*$ and $\mathring{\mathbf{a}}_3$ is the value of $\mathring{\mathbf{a}}_3^*$ for $\theta^3 = 0$. Using the determinant $\mathring{a}^* = |\mathring{a}_{\alpha\beta}^*|$ the volume element of the undeformed laminate reads as:

$$\mathrm{d}\mathring{V} = \sqrt{\mathring{a}^*}\, \mathrm{d}\theta^1\, \mathrm{d}\theta^2\, \mathrm{d}\theta^3. \tag{8}$$

Without the suffix $(\mathring{\ldots})$ the above notations will be used to denote the corresponding geometrical elements of the deformed state. Thus, $\mathbf{a}_\alpha = \mathbf{r}_{,\alpha}$ are the base vectors associated with the deformed position $P$ of $\mathring{P}$. We, however, note that the base vector $\mathbf{a}_3$ and the unit normal vector $\mathbf{n}_3$ are not identical in this case so that an expression similar to (4) in terms of the base vector $\mathbf{a}_3$ does not hold for the curvature tensor $b_{\alpha\beta}$ of the deformed middle surface $F$.

## 3. DEFORMATION STATE

In the following we shall first deal with the description of the refined single-layer theory using the middle surface $\mathring{F}$ as the reference surface. In this theory the position vector $\mathbf{r}^* = \mathbf{r}^*(\theta^i)$ related to an arbitrary point $P^*$ of the deformed laminate is described by the following cubic series expansion in the thickness coordinate $\theta^3$ (Fig. 2):

$$\mathbf{r}^*(\theta^i) = \mathbf{r} + \theta^3 \mathbf{a}_3 + (\theta^3)^2 \mathbf{u} + (\theta^3)^3 \mathbf{y}, \tag{9}$$

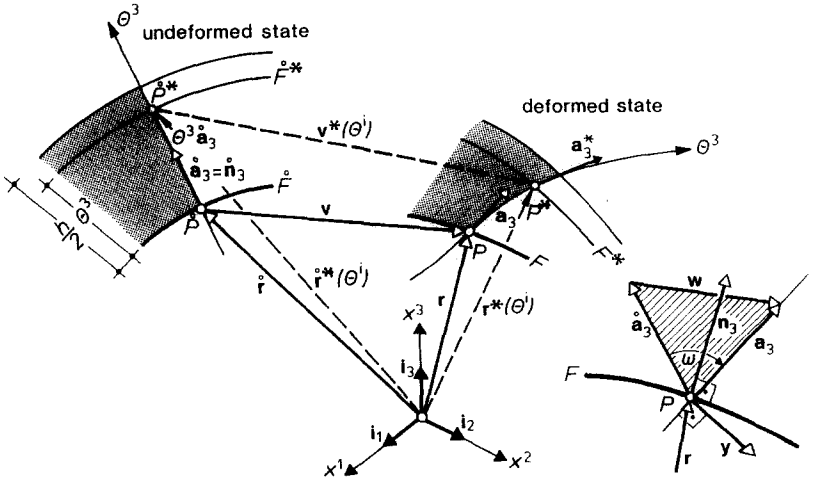


Fig. 2. Definition of displacement variables.

with the unknown 2D variables $\mathbf{r}$, $\mathbf{a}_3$, $\mathbf{u}$ and $\mathbf{y}$. The notation selected in (9) for the first order kinematic variable is in accordance with the fact that $\mathbf{a}_3 = \mathbf{r}^*_{,3}(\theta^3 = 0)$, which is the base vector related to the middle surface $F$. We, however, note that $\mathbf{a}_3$ is not perpendicular to $F$. Introducing the expressions (5) and (9) into the well-known definition of Green's tensor (Green and Zerna, 1968)

$$\gamma_{ij} = \tfrac{1}{2}(\mathbf{r}^*_{,i} \cdot \mathbf{r}^*_{,j} - \mathring{\mathbf{r}}^*_{,i} \cdot \mathring{\mathbf{r}}^*_{,j})$$

and considering (7) we obtain

$$\gamma_{ij} = \begin{bmatrix} \gamma_{\alpha\beta} & \gamma_{\alpha 3} \\ \gamma_{3\alpha} & \gamma_{33} \end{bmatrix} = \begin{bmatrix} \sum\limits_{n=0}^{3} (\theta^3)^n \overset{n}{\gamma}_{\alpha\beta} & \sum\limits_{k=0}^{2} (\theta^3)^k \overset{k}{\gamma}_{\alpha 3} \\ \sum\limits_{k=0}^{2} (\theta^3)^k \overset{k}{\gamma}_{\alpha 3} & \sum\limits_{k=0}^{2} (\theta^3)^k \overset{k}{\gamma}_{33} \end{bmatrix}, \tag{10}$$

where the following 2D strains have been introduced:

$$\begin{aligned}
\overset{0}{\gamma}_{\alpha\beta} &= \tfrac{1}{2}(\mathbf{r}_{,\alpha} \cdot \mathbf{r}_{,\beta} - \mathring{\mathbf{r}}_{,\alpha} \cdot \mathring{\mathbf{r}}_{,\beta}), \\
\overset{1}{\gamma}_{\alpha\beta} &= \tfrac{1}{2}[(\mathbf{a}_{3,\alpha} \cdot \mathbf{r}_{,\beta} + \mathbf{a}_{3,\beta} \cdot \mathbf{r}_{,\alpha}) - (\mathring{\mathbf{a}}_{3,\alpha} \cdot \mathring{\mathbf{r}}_{,\beta} + \mathring{\mathbf{a}}_{3,\beta} \cdot \mathring{\mathbf{r}}_{,\alpha})], \\
\overset{2}{\gamma}_{\alpha\beta} &= \tfrac{1}{2}[(\mathbf{a}_{3,\alpha} \cdot \mathbf{a}_{3,\beta} - \mathring{\mathbf{a}}_{3,\alpha} \cdot \mathring{\mathbf{a}}_{3,\beta}) + (\mathbf{r}_{,\alpha} \cdot \mathbf{u}_{,\beta} + \mathbf{r}_{,\beta} \cdot \mathbf{u}_{,\alpha})], \\
\overset{3}{\gamma}_{\alpha\beta} &= \tfrac{1}{2}[(\mathbf{r}_{,\alpha} \cdot \mathbf{y}_{,\beta} + \mathbf{r}_{,\beta} \cdot \mathbf{y}_{,\alpha}) + (\mathbf{a}_{3,\alpha} \cdot \mathbf{u}_{,\beta} + \mathbf{a}_{3,\beta} \cdot \mathbf{u}_{,\alpha})],
\end{aligned} \tag{11}$$

$$\begin{aligned}
\overset{0}{\gamma}_{\alpha 3} &= \tfrac{1}{2}\mathbf{a}_3 \cdot \mathbf{r}_{,\alpha}, \\
\overset{1}{\gamma}_{\alpha 3} &= \tfrac{1}{2}(\mathbf{a}_3 \cdot \mathbf{a}_{3,\alpha} + 2\mathbf{u} \cdot \mathbf{r}_{,\alpha}), \\
\overset{2}{\gamma}_{\alpha 3} &= \tfrac{1}{2}(\mathbf{a}_3 \cdot \mathbf{u}_{,\alpha} + 2\mathbf{u} \cdot \mathbf{a}_{3,\alpha} + 3\mathbf{y} \cdot \mathbf{r}_{,\alpha}),
\end{aligned} \tag{12}$$

$$\begin{aligned}
\overset{0}{\gamma}_{33} &= \tfrac{1}{2}(\mathbf{a}_3 \cdot \mathbf{a}_3 - 1), \\
\overset{1}{\gamma}_{33} &= 2\mathbf{u} \cdot \mathbf{a}_3, \\
\overset{2}{\gamma}_{33} &= 3\mathbf{a}_3 \cdot \mathbf{y} + 2\mathbf{u} \cdot \mathbf{u}.
\end{aligned} \tag{13}$$

The notation $(\overset{n}{.})$ with $n = 0, 1, 2, 3$ indicates the order of the strains appearing in the series expansions (10). In view of the approximation (9) being of third order, higher order $\theta^3$-terms have been neglected in the derivation of the tangential components $\gamma_{\alpha\beta}$ (10). Consequently, the components $\gamma_{\alpha 3}$ and $\gamma_{33}$ have been approximated in (10) by second-order polynomials since the derivative $\mathbf{r}^*_{,3}$ used in this case is described also by a polynomial only of second order.

Up to now, no constraints have been imposed on the unknown variables entering in the approximation (9). In this sense the above relations are exact within the frame of the kinematic model adopted. Now we first constrain the out of plane strain $\gamma_{33}$ to zero and suppose furthermore the transverse shear deformations $\gamma_{\alpha 3}$ to be distributed symmetrically with respect to the middle surface. The mentioned conditions lead by virtue of (10), (12) and (13) to

$$\overset{0}{\gamma}_{33} = 0 = \tfrac{1}{2}(\mathbf{a}_3 \cdot \mathbf{a}_3 - 1), \qquad \rightarrow \mathbf{a}_3 \cdot \mathbf{a}_{3,\alpha} = 0, \tag{14}$$

$$\overset{1}{\gamma}_{33} = 0 = 2\mathbf{u} \cdot \mathbf{a}_3, \quad \overset{1}{\gamma}_{\alpha 3} = 0 = \mathbf{u} \cdot \mathbf{r}_{,\alpha}, \qquad \rightarrow \mathbf{u} = 0, \tag{15}$$

$$\overset{2}{\gamma}_{33} = 0 = 3\mathbf{a}_3 \cdot \mathbf{y} + 2\mathbf{u} \cdot \mathbf{u}, \qquad \rightarrow \mathbf{a}_3 \cdot \mathbf{y} = 0. \tag{16}$$

Equations (15) implying the previous one (14) indicate the vanishing of the second-order variable **u** which is omitted in the further derivation. This, in turn, is considered in the last relation (16) which presents—together with the first relation given in (14)—the constraints to be satisfied by the unknown variables $\mathbf{a}_3$ and **y**. Accordingly, the present theory possesses seven independent displacement variables and in the following is denoted by the abbreviation RT7.

## 4. KINEMATIC RELATIONS

The definitions (11)–(13) will now be transformed into two mechanically equivalent component relations suitable for isoparametric and classical finite element formulations. This will enable us to develop finite elements of both types on the basis of a single kinematic model. As the isoparametric approach requires kinematic relations where deformed and undeformed states are described by variables of the same type, we note that eqns (11)–(13) are those being suitable for this formulation.

*Classical formulation*

To achieve relations suitable for this purpose we introduce the following displacement variables:

$$\mathbf{v} = \mathbf{r} - \mathring{\mathbf{r}} = v_i \mathring{\mathbf{a}}^i, \quad \mathbf{w} = \mathbf{a}_3 - \mathring{\mathbf{a}}_3 = w_i \mathring{\mathbf{a}}^i, \quad \mathbf{y} = y_i \mathring{\mathbf{a}}^i, \tag{17}$$

which are defined with respect to the undeformed basis $\mathring{\mathbf{a}}^i$. The partial derivatives of eqns (17)

$$\mathbf{v}_{,\alpha} = \varphi_{\alpha i} \mathring{\mathbf{a}}^i, \quad \mathbf{w}_{,\alpha} = \psi_{\alpha i} \mathring{\mathbf{a}}^i, \quad \mathbf{y}_{,\alpha} = \xi_{\alpha i} \mathring{\mathbf{a}}^i \tag{18}$$

lead to the definition of the deformation gradients $\varphi_{ai}$, $\psi_{\alpha i}$ and $\xi_{\alpha i}$ to be used later in the kinematic relations as abbreviations. The variables in question are related to their displacement counterparts in a unified manner, e.g.

$$\varphi_{\alpha\beta} = v_\beta|_\alpha - \mathring{b}_{\alpha\beta} v_3, \quad \varphi_{\alpha 3} = v_{3,\alpha} + \mathring{b}^\lambda_\alpha v_\lambda. \tag{19}$$

The consideration of eqns (17) and (18) in (11)–(13) leads to the kinematic relations summarized in Table 1 where $\delta_{ij}$ is the Kronecker Delta.

For later use, we introduce the rotation vector $\boldsymbol{\Omega}$ being tangential to the middle surface $\mathring{F}$

$$\boldsymbol{\Omega} = \Omega^\alpha \mathring{\mathbf{a}}_\alpha = \frac{\omega}{\sin \omega} \mathring{\mathbf{a}}_3 \times \mathbf{w}, \tag{20}$$

Table 1. Kinematic relations for non-vanishing two-dimensional strains

| Classical formulation | Isoparametric formulation |
|---|---|
| $\overset{0}{\gamma}_{\alpha\beta} = \frac{1}{2}(\varphi_{\alpha\beta} + \varphi_{\beta\alpha} + \varphi_{\alpha\rho}\varphi_\beta^{.\rho} + \varphi_{\alpha 3}\varphi_{\beta 3})$ | $\overset{0}{\gamma}_{\alpha\beta} = \frac{1}{2}(X^i_{,\alpha} X^j_{,\beta} - \mathring{X}^i_{,\alpha} \mathring{X}^j_{,\beta})\,\delta_{ij}$ |
| $\overset{1}{\gamma}_{\alpha\beta} = \frac{1}{2}(\psi_{\alpha\beta} + \psi_{\beta\alpha} - \mathring{b}^\rho_\alpha \varphi_{\beta\rho} - \mathring{b}^\rho_\beta \varphi_{\alpha\rho} + \psi_{\alpha\rho}\varphi_\beta^{.\rho} + \psi_{\beta\rho}\varphi_\alpha^{.\rho} + \psi_{\alpha 3}\varphi_{\beta 3} + \psi_{\beta 3}\varphi_{\alpha 3})$ | $\overset{1}{\gamma}_{\alpha\beta} = \frac{1}{2}(X^i_{,\alpha} A^j_{,\beta} + X^i_{,\beta} A^j_{,\alpha} - \mathring{X}^i_{,\alpha} \mathring{A}^j_{,\beta} - \mathring{X}^i_{,\beta} \mathring{A}^j_{,\alpha})\,\delta_{ij}$ |
| $\overset{2}{\gamma}_{\alpha\beta} = -\frac{1}{2}(\mathring{b}^\rho_\alpha \psi_{\beta\rho} + \mathring{b}^\rho_\beta \psi_{\alpha\rho} - \psi_{\alpha\rho}\psi_\beta^{.\rho} - \psi_{\alpha 3}\psi_{\beta 3})$ | $\overset{2}{\gamma}_{\alpha\beta} = \frac{1}{2}(A^i_{,\alpha} A^j_{,\beta} - \mathring{A}^i_{,\alpha} \mathring{A}^j_{,\beta})\,\delta_{ij}$ |
| $\overset{3}{\gamma}_{\alpha\beta} = \frac{1}{2}(\xi_{\alpha\beta} + \xi_{\beta\alpha} + \varphi_{\alpha\rho}\xi_\beta^{.\rho} + \varphi_{\beta\rho}\xi_\alpha^{.\rho} + \varphi_{\alpha 3}\xi_{\beta 3} + \varphi_{\beta 3}\xi_{\alpha 3})$ | $\overset{3}{\gamma}_{\alpha\beta} = \frac{1}{2}[\mathring{X}^i_{,\rho}(X^j_{,\alpha} y^\rho_{,\beta} + X^j_{,\beta} y^\rho_{,\alpha}) + \mathring{A}^i(X^j_{,\alpha} y^3_{,\beta} + X^j_{,\beta} y^3_{,\alpha}) + y^3(\mathring{A}^i_{,\alpha} X^j_{,\beta} + \mathring{A}^i_{,\beta} X^j_{,\alpha})]\,\delta_{ij}$ |
| $\overset{0}{\gamma}_{\alpha 3} = \frac{1}{2}[w_\lambda(\delta^\lambda_\alpha + \varphi_\alpha^{.\lambda}) + (1 + w_3)\varphi_{\alpha 3}]$ | $\overset{0}{\gamma}_{\alpha 3} = \frac{1}{2} X^i_{,\alpha} A^j\,\delta_{ij}$ |
| $\overset{2}{\gamma}_{\alpha 3} = \frac{1}{2}[y_\lambda(\delta^\lambda_\alpha + \varphi_\alpha^{.\lambda}) + y_3\varphi_{\alpha 3}]$ | $\overset{2}{\gamma}_{\alpha 3} = \frac{1}{2}(\mathring{X}^i_{,\rho} X^j_{,\alpha} y^\rho + \mathring{A}^i X^j_{,\alpha} y^3)\,\delta_{ij}$ |

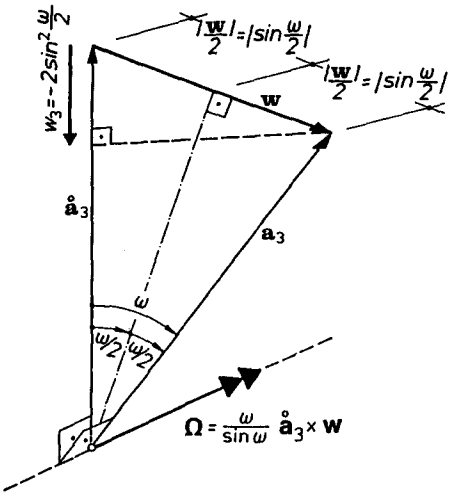


Fig. 3. Rotation vector $\boldsymbol{\Omega}$.

where $\omega$ denotes the rotation angle illustrated in Fig. 3. For the calculation of $\mathbf{w}$ and $\mathbf{a}_3$ in terms of the rotation vector $\boldsymbol{\Omega}$ the following transformations can be used:

$$w_\alpha = \frac{\sin\omega}{\omega}\,\mathring{\varepsilon}_{\alpha\beta}\Omega^\beta, \quad w_3 = \cos\omega - 1 = -2\sin^2\frac{\omega}{2}, \quad \omega = |\boldsymbol{\Omega}| = \sqrt{\Omega^\alpha \Omega_\alpha},$$

$$\mathbf{a}_3 = \mathring{\mathbf{a}}_3 + \frac{\sin\omega}{\omega}\,\boldsymbol{\Omega}\times\mathring{\mathbf{a}}_3 + (\cos\omega - 1)\mathring{\mathbf{a}}_3, \tag{21}$$

which have been obtained from (17) and (20). The relations (21) implying the constraint $|\mathbf{a}_3| = 1$ demonstrate that the difference vector $\mathbf{w}$ is uniquely determined in every deformed state if the tangential rotation vector $\boldsymbol{\Omega}_\alpha$ is given.

By means of (17), the constraint (14) for the variable $\mathbf{a}_3$ takes the form

$$\mathbf{a}_3 \cdot \mathbf{a}_3 - 1 = w_3(2 + w_3) + w_\alpha w^\alpha = 0 \quad \rightarrow w_3 = -1 \pm \sqrt{1 - w_\alpha w^\alpha}, \tag{22}$$

where the negative sign in front of the square root has to be taken for the values $\pi/2 \leqslant \omega \leqslant 3\pi/2$. This nonlinear constraint with double roots for $w_3$ indicates that the variable $\mathbf{w}$ is, in connection with (22), not able to determine the position of the director $\mathbf{a}_3$ by a unique manner in the range $\omega \geqslant \pi/2$. This causes numerical difficulties if $\omega$ approaches the value $\pi/2$.

To make the present formulation accessible to the finite-rotation analysis it is therefore necessary to omit an explicit consideration of the nonlinear constraint (22) using, instead of $w_\alpha$, suitable rotational quantities as primary variables. An efficient procedure for this purpose is the use of the Rodrigues rotation vector $\boldsymbol{\Omega}$ already adopted by many authors (Simo *et al.*, 1990; Başar, 1993; Büchter and Ramm, 1992). In this case the transformations (21) are to be considered to construct the shape functions of the variable $\mathbf{w}$ or $\mathbf{a}_3$ in the finite element implementation. Another very effective possibility used in the present case and the earlier developments (Başar *et al.*, 1992a,b) is to fix the deformed unit vector

$$\mathbf{a}_3 = A^i \mathbf{i}_i \tag{23}$$

with respect to a global Cartesian reference frame $\mathbf{i}_i$ using the Euler angles (Fig. 4) originally proposed by Ramm (1976). The constraints to be satisfied in this case by $\mathbf{w}$ or $\mathbf{a}_3$ are, according to (17) and (23), of the form

$$w_\alpha = (A^i - \mathring{A}^i)\mathring{X}^j_{,\alpha}\,\delta_{ij}, \quad w_3 = A^i \mathring{A}^j \delta_{ij} - 1, \tag{24}$$

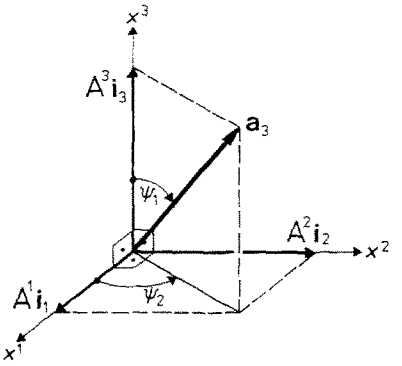


Fig. 4. Definition of rotation variables $\psi_\gamma$.

$$A^1 = \sin\psi_1 \cos\psi_2, \quad A^2 = \sin\psi_1 \sin\psi_2, \quad A^3 = \cos\psi_1. \tag{25}$$

In contrast to (22), the constraint (16) for the displacement $y_3$ is a linear one and causes no numerical difficulties. Its component relation is, by means of (17), given by

$$y_3 = -\frac{1}{1+w_3} w^\alpha y_\alpha, \tag{26}$$

which will be used in the finite element procedure for the elimination of $y_3$ at the element level.

*Isoparametric formulation*

To obtain suitable component relations, the vectors $\mathbf{r}$ and $\mathbf{a}_3$ are now decomposed with respect to a fixed orthogonal Cartesian basis $\mathbf{i}_i$

$$\mathbf{r} = X^i \mathbf{i}_i, \quad \mathbf{a}_3 = A^i \mathbf{i}_i. \tag{27}$$

From the numerical point of view it is convenient to use for the vector $\mathbf{y}$ the earlier decomposition (17) with respect to the middle surface basis $\mathring{\mathbf{a}}_i$. Thus, its consideration together with (27) in the kinematic equations (11)–(13) leads to the component relations (Table 1) to be used in the following finite element formulation. The constraints to be considered in the present case are identical with those given in (25) and (26) where $w_i$ are to be replaced by the expressions (24).

## 5. 2D FORCE VARIABLES AND THE PRINCIPLE OF VIRTUAL WORK

To define 2D force variables being consistent with the strains introduced in (10) we use the internal virtual work of the laminate continuum given in terms of the Piola–Kirchhoff stress tensor of second kind $s^{ij}$ by (Green and Zerna, 1968)

$$\delta^* A_i = -\int\int\int_{\mathring{V}} \mathring{\mu} s^{ij}\, \delta\gamma_{ij} \sqrt{\mathring{a}}\, \mathrm{d}\theta^1\, \mathrm{d}\theta^2\, \mathrm{d}\theta^3, \quad \mathring{\mu} = \sqrt{\mathring{a}^*/\mathring{a}}. \tag{28}$$

Substituting $\gamma_{\alpha\beta}$ and $\gamma_{\alpha 3}$ from (10) and abbreviating the surface element by $\mathrm{d}\mathring{F} = \sqrt{\mathring{a}}\, \mathrm{d}\theta^1\, \mathrm{d}\theta^2$ we obtain, in view of the condition $\gamma_{33} = 0$, the expression

$$\delta^* A_i = -\int\int_{\mathring{F}} \left( \sum_{n=0}^{3} \overset{n}{S}{}^{(\alpha\beta)}\, \delta\overset{n}{\gamma}_{\alpha\beta} + 2 \sum_{m=0,2} \overset{m}{S}{}^{\alpha 3}\, \delta\overset{m}{\gamma}_{\alpha 3} \right) \mathrm{d}\mathring{F}, \tag{29}$$

where the consistent force variables

$$\overset{n}{S}{}^{(\alpha\beta)} = \int_{-h/2}^{+h/2} \mathring{\mu} s^{\alpha\beta} (\theta^3)^n \, \mathrm{d}\theta^3, \quad n = 0, 1, 2, 3,$$

$$\overset{m}{S}{}^{\alpha 3} = \int_{-h/2}^{+h/2} \mathring{\mu} s^{\alpha 3} (\theta^3)^m \, \mathrm{d}\theta^3, \quad m = 0, 2, \tag{30}$$

are similar to the corresponding strains, denoted by $(\overset{n}{.}.)$. In view of the well-known symmetry $s^{ij} = s^{ji}$, the 2D force variables (30) are symmetric which is indicated by round brackets. The above force variables are geometrically not interpretable on the middle surface element and present in this sense pseudo-variables (Başar, 1987).

As external forces we consider surface loads $\sqrt{a/\mathring{a}}\,\mathbf{p}$ per unit area of the undeformed middle surface $\mathring{F}$ and the line loads $(\mathrm{d}s/\mathrm{d}\mathring{s})\mathbf{n}$ per unit length of the boundary curve $\mathring{C}$ of the undeformed middle surface. Thus, the principle of virtual work can, considering (29), be expressed as

$$\delta^* A = \delta^* A_a + \delta^* A_i = 0 = \int\int_{\mathring{F}} \left( \sqrt{\frac{a}{\mathring{a}}}\, \mathbf{p} \right) \cdot \delta \mathbf{v} \, \mathrm{d}\mathring{F} + \int_{\mathring{C}} \left( \frac{\mathrm{d}s}{\mathrm{d}\mathring{s}} \mathbf{n} \right) \cdot \delta \mathbf{v} \, \mathrm{d}\mathring{s}$$

$$- \int\int_{\mathring{F}} \left( \sum_{n=0}^{3} \overset{n}{S}{}^{(\alpha\beta)} \delta \overset{n}{\gamma}_{\alpha\beta} + 2 \sum_{m=0,2} \overset{m}{S}{}^{\alpha 3} \delta \overset{m}{\gamma}_{\alpha 3} \right) \mathrm{d}\mathring{F}. \tag{31}$$

## 6. CONSTITUTIVE RELATIONS

We consider a laminate consisting of $N$ laminae made of arbitrary orthotropic material. In each lamina the principal material axes are allowed to be oriented differently with respect to the curvilinear laminate coordinates $\theta^\alpha$. Assuming a zero stress condition $s^{33} = 0$ across the thickness the constitutive equations valid for this case are given by

$$\overset{n}{S}{}^{(\alpha\beta)} = \sum_{j=0}^{3} \overset{j+n}{C}{}^{\alpha\beta\rho\lambda} \overset{j}{\gamma}_{\rho\lambda}, \quad n = 0, 1, 2, 3,$$

$$\overset{m}{S}{}^{\alpha 3} = \sum_{i=0,2} \overset{i+m}{C}{}^{\alpha\rho} \overset{i}{\gamma}_{\rho 3}, \quad m = 0, 2, \tag{32}$$

where

$$\overset{k}{C}{}^{\alpha\beta\rho\lambda} = \sum_{L=1}^{N} \int_{h_{L-1}}^{h_L} \mathring{\mu} C_L^{\alpha\beta\rho\lambda} (\theta^3)^k \, \mathrm{d}\theta^3, \quad k = 0, 1, 2, \ldots, 6,$$

$$\overset{l}{C}{}^{\alpha\rho} = \sum_{L=1}^{N} \int_{h_{L-1}}^{h_L} \mathring{\mu} C_L^{\alpha\rho} (\theta^3)^l \, \mathrm{d}\theta^3, \quad l = 0, 2, 4 \tag{33}$$

and the index $L$ characterizes variables referring to the $L$th layer. The relations, which permit a pointwise determination of the tensorial elastic coefficients $C_L^{\alpha\beta\rho\lambda}$ and $C_L^{\alpha\rho}$ in terms of the given material properties and the ply angle $\alpha$, are given with a detailed derivation in Başar (1993). To reduce computational efforts the thickness integration in (33) is performed in the numerical implementation for each lamina explicitly, approximating the metric tensor $a^{*\alpha\beta}$ of the laminate continuum by that of the reference surface $a^{\alpha\beta}$.

## 7. SPECIAL CASES

By introducing additional kinematic constraints for the unknown variables entering in the approximation (9) the above third order theory can easily be transformed into three simplified models which are to be denoted in the following by the notations given in Table

Table 2. Notations for the different single-layer theoretical models

| | RT7 | RT5 | T5 | T3 |
|---|---|---|---|---|
| Internal virtual work | $\delta^* A_i = -\int\int_F \left( \sum_{n=0}^{3} \overset{n}{S}^{(\alpha\beta)} \delta \overset{n}{\gamma}_{\alpha\beta} + \sum_{m=0,2} \overset{m}{S}^{\alpha} \delta \overset{m}{\gamma}_{\alpha} \right) dF$ | | | |
| Independent displacements | $v_i, \psi_\alpha, y_3$ | $v_i, \psi_\alpha$ | $v_i, \psi_\alpha$ | $v_i$ |
| Existing two-dimensional strains | $\overset{n}{\gamma}_{\alpha\beta}$ $(n = 0, 1, 2, 3)$<br>$\overset{m}{\gamma}_{\alpha 3}$ $(m = 0, 2)$ | $\overset{n}{\gamma}_{\alpha\beta}$ $(n = 0, 1, 2, 3)$<br>$\overset{0}{\gamma}_{\alpha 3} = -\frac{h^2}{4} \overset{2}{\gamma}_{\alpha 3} = \frac{1}{2}\gamma_\alpha$ | $\overset{0}{\gamma}_{\alpha\beta} = \alpha_{\alpha\beta}$<br>$\overset{1}{\gamma}_{\alpha\beta} = \beta_{\alpha\beta}$<br>$\overset{0}{\gamma}_{\alpha 3} = \frac{1}{2}\gamma_\alpha$ | $\overset{0}{\gamma}_{\alpha\beta} = \alpha_{\alpha\beta}$<br>$\overset{1}{\gamma}_{\alpha\beta} = \omega_{\alpha\beta}$ |
| Displacements in kinematic relations | $v_i, w_i, y_i$ | $v_i, w_i, y_i$ | $v_i, w_i$ | $v_i, w_i$ |
| Constraints for displacements | $w_i = w_i(\psi_\alpha)$<br>$y_3 = y_3(w_i, y_\alpha)$ | $w_i = w_i(\psi_\alpha)$<br>$y_3 = y_3(w_i, y_\alpha)$<br>$y_\alpha = y_\alpha(v_i, w_i)$ | $w_i = w_i(\psi_\alpha)$ | $w_i = w_i(v_i)$ |

2. Already at this stage we note that the constraint (14) for **w** preserves its validity in all cases. Only in the Kirchhoff–Love type theory will it be augmented by two further conditions. The constraint (16) for **y** is significant only for the first special case and need not be considered in the other models where **y** does not occur. This short discussion clearly shows that all the models presented in this paper differ from each other mainly by the constraints to be satisfied by the displacement variables: a significant advantage for the numerical implementation.

*Refined theory with five independent displacement variables (RT5)*

In this case the shear strains $\gamma_{\alpha 3}$ are supposed to vanish on the laminate faces $\theta^3 = \pm h/2$. Using (10) and the relations from Table 1, this may be expressed as

$$\overset{2}{\gamma}_{\alpha 3} = -\frac{4}{h^2} \overset{0}{\gamma}_{\alpha 3} = \tfrac{3}{2}[y_\lambda(\delta^\lambda_\alpha + \varphi_{\alpha,}{}^\lambda) + y_3 \varphi_{\alpha 3}]$$
$$= \tfrac{3}{2}(\mathring{X}^i_{,\rho} X^j_{,\alpha} y^\rho + \mathring{A}^i X^j_{,\alpha} y^3)\, \delta_{ij}. \tag{34}$$

This equation permits the elimination of the second-order shear strains $\overset{2}{\gamma}_{\alpha 3}$ and by considering additionally (26) also the third-order displacement vector **y**, which becomes in the present case a purely dependent variable. The second-order shear strains $\overset{2}{\gamma}_{\alpha 3}$ are now to be calculated according to the conditions (34) while the kinematic relations of all other strains can be adopted again from Table 1. The main characteristics of this model and the following ones are summarized in Table 2. Finally, we note that the present model reduces for the linear analysis of plates to that proposed by Reddy (1984).

*Mindlin–Reissner type theory (T5)*

This model supposes a constant distribution of shear strains $\gamma_{\alpha 3}$ across the thickness. This requirement leads by considering (10)–(12) and (15), (16) to the vanishing of the following variables:

$$\overset{2}{\gamma}_{\alpha 3} = 0, \quad \overset{3}{\gamma}_{\alpha\beta} = 0, \quad y_i = 0. \tag{35}$$

This, in turn, justifies a further simplification $\overset{2}{\gamma}_{\alpha\beta} = 0$ (Başar and Krätzig, 1985) so that the deformation state is governed only by the variables $\alpha_{\alpha\beta} = \overset{0}{\gamma}_{\alpha\beta}$, $\beta_{\alpha\beta} = \overset{1}{\gamma}_{\alpha\beta}$ and $\gamma_\alpha = 2\overset{0}{\gamma}_{\alpha 3}$, the kinematic relations of which can be adopted from Table 1. For the isotropic case this model corresponds exactly to that presented in Başar (1987).

*Kirchhoff–Love type theory (T3)*

This model can be obtained from the previous one by assuming that $\overset{0}{\gamma}_{\alpha 3} = 0$. This yields by virtue of (12), (17) and (18) the following orthogonality relation:

$$\overset{0}{\gamma}_{\alpha 3} = \tfrac{1}{2}\mathbf{a}_3 \cdot \mathbf{a}_\alpha = 0 = \tfrac{1}{2}[(\delta_\alpha^\rho + \varphi_\alpha{}^\rho)w_\rho + \varphi_{\alpha 3}(1+w_3)], \tag{36}$$

forming together with (22) a complete set of equations for the elimination of the dependent variable $\mathbf{w}$. The numerical procedure to be used for an exact enforcement of the Kirchhoff–Love hypothesis (22), (36) as well as further useful details of this model are given for the isotropic case in earlier works (Başar and Ding, 1990; Ding, 1989).

## 8. THE GEOMETRICAL INTERPRETATION OF FORCE VARIABLES

The force variables (30) have been introduced by a variational procedure and are, consequently, geometrically not interpretable on the middle surface element. To make the theory accessible for practical applications we shall relate them in the following to geometrically interpretable ones which are to be introduced directly on the 2D shell element (Başar and Krätzig, 1985). For this purpose we consider an element of the deformed coordinate line $\theta^\alpha = \text{const.}$, of the length $\mathrm{d}s_{\langle\beta\rangle} = \sqrt{a_{\beta\beta}}\,\mathrm{d}\theta^\beta$ and denote the stress resultant vector acting on it by $\mathbf{n}^\alpha\sqrt{a}\,\mathrm{d}\theta^\beta$ and the corresponding stress couple resultant by $\mathbf{m}^\alpha\sqrt{a}\,\mathrm{d}\theta^\beta$. By the well-known procedure (Başar and Krätzig, 1985) these resultant vectors can be expressed in terms of the stresses $s^{ij}$, the results being of the form:

$$\begin{aligned}
\sqrt{\frac{a}{\mathring{a}}}\,\mathbf{n}^\alpha &= \int_{-h/2}^{h/2} \mathring{\mu} s^{\alpha i}\mathbf{a}_i^*\,\mathrm{d}\theta^3,\\
\sqrt{\frac{a}{\mathring{a}}}\,\mathbf{m}^\alpha &= \int_{-h/2}^{h/2} \mathring{\mu} s^{\alpha i}\theta^3(\mathbf{a}_3 + (\theta^3)^2\mathbf{y}) \times \mathbf{a}_i^*\,\mathrm{d}\theta^3.
\end{aligned} \tag{37}$$

Expressing the base vectors $\mathbf{a}_i^*$ according to the kinematic assumption (9) yields in view of the definitions (30)

$$\begin{aligned}
\sqrt{\frac{a}{\mathring{a}}}\,\mathbf{n}^\alpha &= \overset{0}{S}{}^{(\alpha\beta)}\mathbf{a}_\beta + \overset{1}{S}{}^{(\alpha\beta)}\mathbf{a}_{3,\beta} + \overset{3}{S}{}^{(\alpha\beta)}\mathbf{y}_{,\beta} + \overset{0}{S}{}^{\alpha 3}\mathbf{a}_3 + 3\overset{2}{S}{}^{\alpha 3}\mathbf{y},\\
\sqrt{\frac{a}{\mathring{a}}}\,\mathbf{m}^\alpha &= \overset{1}{S}{}^{(\alpha\beta)}\mathbf{a}_3 \times \mathbf{a}_\beta + \overset{2}{S}{}^{(\alpha\beta)}\mathbf{a}_3 \times \mathbf{a}_{3,\beta} + \overset{3}{S}{}^{(\alpha\beta)}\mathbf{y} \times \mathbf{a}_\beta,
\end{aligned} \tag{38}$$

where all terms connected with force variables being of higher order than the consistent ones (30) have been neglected. The resultant vectors (37) are now used to define the following geometrical interpretable force variables:

$$\begin{aligned}
\sqrt{\frac{a}{\mathring{a}}}\,\mathbf{n}^\alpha &= N^{\alpha\beta}\mathbf{a}_\beta + Q^\alpha\mathbf{a}_3 = n^{\alpha\beta}\mathring{\mathbf{a}}_\beta + q^\alpha\mathring{\mathbf{a}}_3,\\
\sqrt{\frac{a}{\mathring{a}}}\,\mathbf{m}^\alpha &= M^{\alpha\beta}\mathbf{a}_3 \times \mathbf{a}_\beta + M^\alpha\mathbf{a}_3 = m^{\alpha\beta}\mathring{\mathbf{a}}_3 \times \mathring{\mathbf{a}}_\beta + m^\alpha\mathring{\mathbf{a}}_3.
\end{aligned} \tag{39}$$

The first ones related to the deformed basis (Piola–Kirchhoff force variables of the second kind) are relevant for the evaluation of the real force distribution in the deformed shell continuum. The force variables denoted by lower-case letters $n^{\alpha\beta}, q^\alpha, \ldots$ are the Lagrangian ones defined with respect to the undeformed basis $\mathring{\mathbf{a}}_i$.

Using (17) and (18), eqns (38) and (39) can easily be transformed to obtain the relations

Table 3. Different types of force variables and transformations

| | |
|---|---|
| Variationally defined force variables | $\overset{n}{S}{}^{(\alpha\beta)}$ $(n=0,1,2,3)$ $\quad \overset{m}{S}{}^{(\alpha 3)}$ $(m=0,2)$ |
| Piola–Kirchhoff force variables of second kind | $\sqrt{\frac{a}{\mathring{a}}}\,\mathbf{n}^{\alpha}=N^{\alpha\beta}\mathbf{a}_{\beta}+Q^{\alpha}\mathbf{a}_3,\quad \sqrt{\frac{a}{\mathring{a}}}\,\mathbf{m}^{\alpha}=M^{\alpha\beta}\mathbf{a}_3\times\mathbf{a}_{\beta}+M^{\alpha}\mathbf{a}_3$ |
| Lagrangian force variables | $\sqrt{\frac{a}{\mathring{a}}}\,\mathbf{n}^{\alpha}=n^{\alpha\beta}\mathring{\mathbf{a}}_{\beta}+q^{\alpha}\mathring{\mathbf{a}}_3,\quad \sqrt{\frac{a}{\mathring{a}}}\,\mathbf{m}^{\alpha}=m^{\alpha\beta}\mathring{\mathbf{a}}_3\times\mathring{\mathbf{a}}_{\beta}+m^{\alpha}\mathring{\mathbf{a}}_3$ |

Transformations

$$n^{\alpha\beta}=(\delta^{\beta}_{\rho}+\varphi_{\rho}{}^{\beta})\overset{0}{S}{}^{(\alpha\rho)}-(\overset{\circ}{b}{}^{\beta}_{\rho}-\psi_{\rho}{}^{\beta})\overset{1}{S}{}^{(\alpha\rho)}+\xi_{\rho}{}^{\beta}\overset{3}{S}{}^{(\alpha\rho)}+w^{\beta}\overset{0}{S}{}^{(\alpha 3)}+3y^{\beta}\overset{2}{S}{}^{(\alpha 3)}$$

$$q^{\alpha}=(1+w_3)\overset{0}{S}{}^{(\alpha 3)}+3y_3\overset{2}{S}{}^{(\alpha 3)}+\varphi_{\beta 3}\overset{0}{S}{}^{(\alpha\beta)}+\psi_{\beta 3}\overset{1}{S}{}^{(\alpha\beta)}+\xi_{\beta 3}\overset{3}{S}{}^{(\alpha\beta)}$$

$$m^{\alpha\beta}=(1+w_3)\left(\delta^{\beta}_{\lambda}+\varphi_{\lambda}{}^{\beta}-\frac{w^{\beta}}{1+w_3}\varphi_{\lambda 3}\right)\overset{1}{S}{}^{(\alpha\lambda)}-(1+w_3)\left(\overset{\circ}{b}{}^{\beta}_{\lambda}-\psi_{\lambda}{}^{\beta}+\frac{w^{\beta}}{1+w_3}\psi_{\lambda 3}\right)\overset{2}{S}{}^{(\alpha\lambda)}+y_3\left(\delta^{\beta}_{\lambda}+\varphi_{\lambda}{}^{\beta}-\frac{y^{\beta}}{y_3}\varphi_{\lambda 3}\right)\overset{3}{S}{}^{(\alpha\lambda)}$$

$$m_{\alpha}=[w^{\rho}(\delta^{\lambda}_{\beta}+\varphi_{\beta}{}^{\lambda})\overset{1}{S}{}^{(\alpha\beta)}-w^{\rho}(\overset{\circ}{b}{}^{\lambda}_{\beta}-\psi_{\beta}{}^{\lambda})\overset{2}{S}{}^{(\alpha\beta)}+y^{\rho}(\delta^{\lambda}_{\beta}+\varphi_{\beta}{}^{\lambda})\overset{3}{S}{}^{(\alpha\beta)}]\mathring{\varepsilon}_{\rho\lambda}$$

$$n^{\alpha\beta}=(\delta^{\beta}_{\rho}+\varphi_{\rho}{}^{\beta})N^{\alpha\rho}+Q^{\alpha}w^{\beta}$$

$$q^{\alpha}=(1+w_3)Q^{\alpha}+\varphi_{\rho 3}N^{\alpha\rho}$$

$$m^{\alpha\beta}=(1+w_3)\left(\delta^{\beta}_{\lambda}+\varphi_{\lambda}{}^{\beta}-\frac{w^{\beta}}{1+w_3}\varphi_{\lambda 3}\right)M^{(\alpha\lambda)}+w_{\rho}\mathring{\varepsilon}^{\beta\rho}M^{\alpha}$$

$$m^{\alpha}=w^{\rho}(\delta^{\lambda}_{\beta}+\varphi_{\beta}{}^{\lambda})M^{(\alpha\beta)}\mathring{\varepsilon}_{\rho\lambda}+(1+w_3)M^{\alpha}$$

given in Table 3. These relations permit the calculation of the geometrically interpretable variables $N^{\alpha\beta}$, $Q^{\alpha}$—by solving a linear equation system in the finite element procedure—in terms of those introduced by a variational procedure (30). The transformation of the tensorial components $N^{\alpha\beta}$, $Q^{\alpha}$, ... into the physical ones $N^{\langle\alpha\beta\rangle}$, $Q^{\langle\alpha\rangle}$, ... presenting variables per unit length of the deformed coordinate lines $\theta^{\alpha}=\text{const.}$ can finally be accomplished by the well-known relations given, e.g. in Başar and Ding (1990).

## 9. A LAYER-WISE THEORY

In all single-layer theories presented above, the displacement field of the laminate is described by a single series expansion through the thickness, possessing at least $C^1$-continuity. Consequently, the shear deformations are continuous across the thickness. Such theoretical models therefore are not able to simulate laminates made of dissimilar material layers with sufficient accuracy. This particularly concerns the prediction of local effects such as interlaminar stress distributions and delaminations. To eliminate this deficiency a layer-wise theory can be used.

The basic concepts of this model can be summarized as follows: First, the given structure is subdivided into $N$ sub-elements across the thickness such that at least one sub-element per layer is used. Each sub-element is then described by the Mindlin–Reissner type theory T5. Finally, a $C^0$-displacement continuity condition is imposed on the laminate displacement field leading to a theoretical model with $2N+3$ independent displacement variables in the case of $N$ sub-elements across the thickness.

We now consider a laminate sub-divided into $N$ sub-elements (Fig. 5). To formulate the relations referred to the sub-element $L$ we shall use its middle surface

$$\xi^3=\frac{1}{2}\sum_{J=1}^{L-1}(h_J+h_{J+1})$$

as reference surface $\mathring{F}_L$ and the middle surface of the first sub-element ($\xi^3=0$) as reference surface $\mathring{F}_1$ of the whole laminate. This selection is advantageous since the layer-wise theory becomes identical with the Mindlin–Reissner type theory if the structure is treated by a single sub-element. The use of the middle surface as reference surface is also suitable to minimize

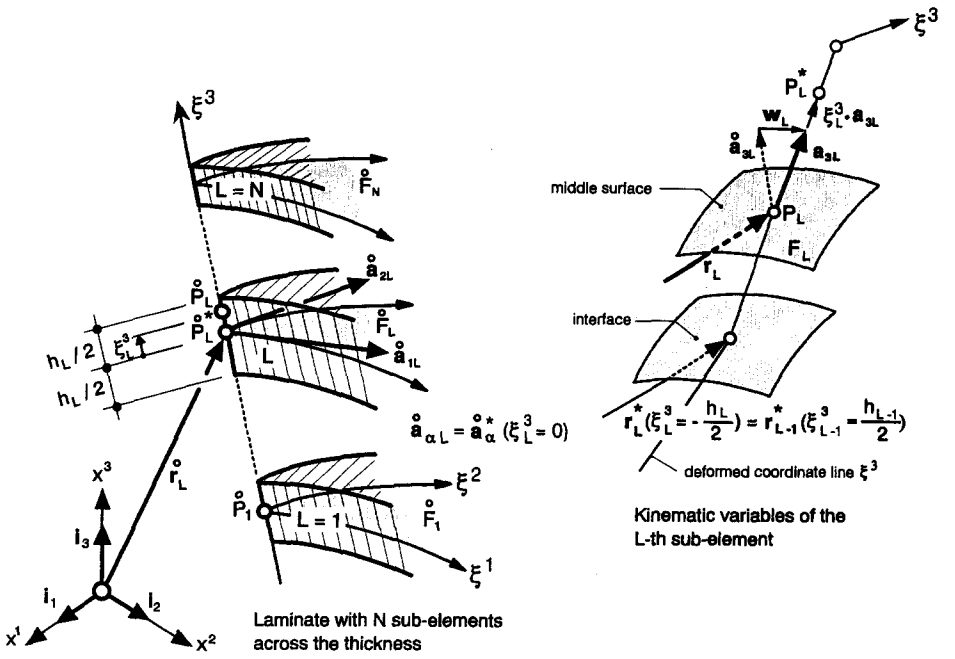


Fig. 5. Laminate with $N$ sub-elements across the shell thickness.

errors in constructing the laminate elasticity tensor (33). In each lamina the metric tensor $a^*_{\alpha\beta L}$ of the lamina continuum will be approximated by that of its reference surface $a_{\alpha\beta L}$ to perform the thickness integration explicitly.

The geometrical variables of the sub-element $L$ can be calculated again according to Section 2. Using the index $(\ldots)_L$ to characterize the associated variables we find, e.g. from (6) for the base vectors $\mathring{\mathbf{a}}^*_{\alpha L}$ of an arbitrary point $\mathring{P}^*_L(-(h_L/2) \leqslant \xi^3_L \leqslant (h_L/2))$

$$\mathring{\mathbf{a}}^*_{\alpha L} = \mathring{\mathbf{r}}^*_{L,\alpha} = \mathring{\mathbf{a}}_{\alpha L} + \xi^3_L \mathring{\mathbf{a}}_{3,\alpha} = \mathring{\mathbf{a}}_{\alpha 1} + \xi^3 \mathring{\mathbf{a}}_{3,\alpha} = (\mathring{X}^i_{L,\alpha} + \xi^3_L \mathring{A}^i_{,\alpha})\mathbf{i}_i, \tag{40}$$

where $\xi^3$ and $\xi^3_L$ indicate the distance of the point $\mathring{P}^*_L$ from the surfaces $\mathring{F}_1$ and $\mathring{F}_L$, respectively, measured in $\mathring{\mathbf{a}}_3 = \mathring{\mathbf{a}}_{3L}$ direction. In the following, equations will be presented as in (40) in isoparametric form. The other geometrical elements of Section 2 can be specialized similarly on the sub-element $L$.

Within the frame of the Mindlin–Reissner type theory T5 the position vector $\mathbf{r}^*_L$ of an arbitrary point $P^*_L$ of the deformed sub-element $L$ is described by the linear approximation

$$\mathbf{r}^*_L = \mathbf{r}_L + \xi^3_L \mathbf{a}_{3L} \tag{41}$$

with the 2D vectors $\mathbf{r}_L$ and $\mathbf{a}_{3L}$ to be decomposed with respect to the global Cartesian coordinate system $\mathbf{i}_i$:

$$\mathbf{r}_L = X^i_L \mathbf{i}_i, \quad \mathbf{a}_{3L} = A^i_L \mathbf{i}_i. \tag{42}$$

In contrast to the single-layer theory T5 the position vector $\mathbf{r}_L$ introduced in eqn (41) is a dependent variable. If we require the position vectors $\mathbf{r}^*_L$ $(L = 2, \ldots, N)$ to satisfy the $C^0$-continuity condition

$$\mathbf{r}^*_L\left(\xi^3_L = -\frac{h_L}{2}\right) = \mathbf{r}^*_{L-1}\left(\xi^3_{L-1} = \frac{h_{L-1}}{2}\right) \tag{43}$$

on all interfaces between two adjacent sub-elements we find for the position vector $\mathbf{r}_L$, by

means of eqn (41), the following expression:

$$\mathbf{r}_L = \mathbf{r}_{L-1} + \tfrac{1}{2}(h_{L-1}\mathbf{a}_{3L-1} + h_L\mathbf{a}_{3L}) = \mathbf{r}_1 + \frac{1}{2}\sum_{J=1}^{L-1}(h_J\mathbf{a}_{3J} + h_{J+1}\mathbf{a}_{3J+1}). \tag{44}$$

In view of (42) eqn (44) can be rewritten in terms of the components $X^i_J$ resp. $X^i_1$ and $A^i_J$ as:

$$X^i_L = X^i_{L-1} + \tfrac{1}{2}(h_{L-1}A^i_{L-1} + h_L A^i_L) = X^i_1 + \frac{1}{2}\sum_{J=1}^{L-1}(h_J A^i_J + h_{J+1}A^i_{J+1}). \tag{45}$$

Relation (44) indicates that the position vector $\mathbf{r}_L$ ($L = 2, \ldots, N$) depends on the position vector $\mathbf{r}_1$ of the first sub-element and the deformed directors $\mathbf{a}_{3J}$ of all foregoing sub-elements $J$ from 1 to $L$, so that eqn (45) can be employed for the elimination of $X^i_L$ at the element level. It is obvious that the first relation in (45) is computationally more efficient than the second one in the case of a large number of sub-elements. Consequently it has been used in the numerical implementation. Also in the present theory, the vector $A^i_J$ ($J = 1, \ldots, L$) is to be transformed into the independent rotational variables $\psi_{\alpha L}$ in order to satisfy the constraint $a_{3L} \cdot \mathbf{a}_{3L} = 1$ *a priori*.

The deformation state of the sub-element $L$ is described by the tangential strains $\alpha_{\alpha\beta L} = \overset{0}{\gamma}_{\alpha\beta L}$, $\beta_{\alpha\beta L} = \overset{1}{\gamma}_{\alpha\beta L}$ and the shear strains $\gamma_{\alpha L} = 2\overset{0}{\gamma}_{\alpha 3L}$. The kinematic relations of isoparametric form summarized in Table 1 can easily be specialized for the sub-element $L$ replacing the variables $X^i$ and $A^i$ by $X^i_L$ and $A^i_L$, e.g.

$$\alpha_{\alpha\beta L} = \tfrac{1}{2}(X^i_{L,\alpha}X^j_{L,\beta} - \mathring{X}^i_{L,\alpha}\mathring{X}^j_{L,\beta})\,\delta_{ij}. \tag{46}$$

Thus, the internal virtual work given in (29) for a single-layer theory can be generalized to the present case as follows:

$$\delta^* A_i = -\sum_{L=1}^{N}\int\!\!\int_{\mathring{F}_1}\sqrt{\frac{\mathring{a}_L}{\mathring{a}_1}}\,(\mathring{S}^{(\alpha\beta)}_L\,\delta\alpha_{\alpha\beta L} + \mathring{S}^{(\alpha 3)}_L\,\delta\gamma_{\alpha L} + \overset{1}{\mathring{S}}{}^{(\alpha\beta)}_L\,\delta\beta_{\alpha\beta L})\,\mathrm{d}\mathring{F}_1, \tag{47}$$

where the multiplier $\sqrt{\mathring{a}_L/\mathring{a}_1}$ indicates the surface integration to be performed over the reference surface $\mathring{F}_1$ of the first sub-element.

## 10. FINITE-ELEMENT FORMULATION

For the application of an incremental-iterative solution strategy the nonlinear equations presented above are transformed according to a variational procedure [see, e.g. Başar and Krätzig (1985) and Başar and Ding (1990)] into incremental equations where all fundamental state quantities are evaluated by the exact nonlinear relations. The basic concepts used in the development of shear deformation models can be summarized as follows: Interpolation polynomials are introduced directly for the rotational variables $\psi_\alpha$, but not for the director $\mathbf{a}_3$. This provides an exact enforcement of the constraint $\mathbf{a}_3 \cdot \mathbf{a}_3 = 1$ on the whole finite element area. Thus the finite elements developed present, according to the classification proposed by Büchter (1992), shell theory elements and not degenerated ones. Constraints existing for all dependent kinematic quantities are considered at the element level numerically.

Finite element models developed by means of the above theoretical models can be summarized as follows:

LWT-IAS4: layer-wise theory LWT, 4-node isoparametric assumed strain element

Table 4. Isoparametric assumed strain finite-rotation shell elements based on the third-order theory RT7 and the layer-wise theory LWT

| | Isoparametric Assumed Strain Finite-Rotation Elements | |
|---|---|---|
| | RT7-IAS4 | LWT-IAS4 |
| | 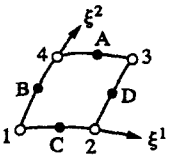 | |
| Theoretical fundamentals | Third order theory (RT7) | Layer-wise theory (LWT) |
| Degrees of freedom | $\Delta X^i$, $\Delta\psi_\alpha$, $y^\alpha$ (7 x 4) | $\Delta X_1^i$, $\Delta\psi_{\alpha L}$, $L = 1, 2, \ldots, N$ $N$: number of sub-elements across the thickness $(2N + 3)$ x 4 |
| Interpolations for | $\Delta X^i$, $\Delta\psi_\alpha$, $y^\alpha$ | $\Delta X_1^i$, $\Delta\psi_{\alpha L}$, $L = 1, 2, \ldots, N$ |
| | bilinear polynomials | |
| Integration points | 2 x 2 | 2 x 2 |
| Interpolations for $\overset{0}{\bar{\gamma}}_\alpha$ or $\bar{\gamma}_{\alpha L}$ | $\bar{\gamma}_{1L} = \xi^2\gamma_{1L}^A + (1-\xi^2)\gamma_{1L}^C$ $\bar{\gamma}_{2L} = \xi^1\gamma_{2L}^D + (1-\xi^1)\gamma_{2L}^B$ | |

RT7-IAS4: Third order theory RT7, 4-node isoparametric assumed strain element

T5-IAS4: Mindlin–Reissner type theory T5, 4-node isoparametric assumed strain element

T5-M4, M9: Mindlin–Reissner type theory T5, 4-node and 9-node mixed elements

T3-D3, D4: Kirchhoff–Love type theory T3, displacement-based triangular and quadrilateral elements.

Both refined theoretical models LWT and RT7 are transformed into 4-node isoparametric elements. To avoid locking the constant shear deformation term $\overset{0}{\gamma}_{\alpha 3}$ is interpolated in RT7-IAS4 by the assumed strain concept (Dvorkin and Bathe, 1984). Interpolations used for this purpose are presented in Table 4. It has been shown that higher order shear strains $\overset{2}{\gamma}_{\alpha 3}$ occurring in RT7 require no special treatment in this sense. All shear deformation terms $\gamma_{\alpha L}$ $(L = 1, \ldots, N)$ occurring in the layer-wise theory (47) are interpolated in the same manner as $\overset{0}{\gamma}_{\alpha 3}$ in the model RT7. In both refined models the independent displacement variables are interpolated by standard bilinear polynomials. Further characteristics of these models such as integration points are summarized in Table 4. We finally note that the layer-wise model LWT-IAS4 degenerates to the Mindlin–Reissner type model if a single sub-element is used in the analysis.

Mixed models based on the Mindlin–Reissner type theory are described for the isotropic case in Başar *et al.* (1992a) while the works by Başar and Ding (1990) and Ding (1989) contain a detailed presentation of the Kirchhoff–Love type element again for the isotropic case.

## 11. NUMERICAL EXAMPLES

Extended numerical studies have been carried out by the finite-element models described above. First two linear examples will be presented to show the influence of

different theoretical models on the responses for different conditions concerning the side-length to thickness ratio $a/h$ or the modular ratio $R$ which characterizes the layer material dissimilarities. Corresponding parametric studies will permit the discovery of the applicability ranges of different analysis models and the demonstration of the performance of refined models in dealing with extreme situations.

*Linear examples*

*Example 1: Sandwich plate under sinusoidal transverse loads (Pandya and Kant, 1988).* The structure (Fig. 6) is simply supported along all edges and consists of three layers placed symmetrically with respect to the middle surface. The face sheet material is decisively much stiffer than that of the core. This, however, causes no significant discrepancies between the results of different analysis models if the structure is sufficiently thin ($a/h \leqslant 1/100$). This example has been analysed by all finite element models for different values of the thickness $h = 0.01, 0.02, 0.04, 0.10, 0.25$. The results obtained for the deflection $v_{3\max}(\theta^1, \theta^2 = a/2)$ and the stresses $s^{\alpha\alpha}(\theta^1, \theta^2 = a/2,\ \theta^3 = h/2,\ 4h/10)$, $s^{12}(\theta^1 = a/2,\ \theta^2 = 0,\ \theta^3 = h/2)$ are nondimensionalized by the multipliers

$$m_1 = \frac{100h^3}{pa^4} E_2 \text{ (face sheets)}, \quad m_2 = \frac{h^2}{pa^2}.$$

For a precise comparison some characteristic values obtained by using $16 \times 16$ shear deformation elements or $5 \times 5$ T3-D4 elements per one quarter of the plate are summarized in Table 5. In Figs 7 and 8 numerical results for the deflection $v_3(\theta^1 = \theta^2 = a/2)$ and the normal stresses $s^{11}(\theta^1 = \theta^2 = a/2,\ \theta^3 = h/2)$ are plotted versus the parameter $a/h$ showing the different accuracy levels of the models used in the analysis. We note that the normal stresses $s^{11}$ are, due to the selected lamination scheme, of higher order of magnitude than the normal stresses $s^{22}$ and thus for a comparative study more relevant.

From Figs 7 and 8 it can easily be seen that the numerical results obtained by the refined models RT7 and LWT and those calculated by Pandya and Kant (1988) by a theoretical model similar to RT7 agree very well within a large range of the investigated region $a/h$. Significant discrepancies between the results due to the model RT7 and the layer-wise model LWT occur for very thick structures ($a/h \leqslant 4$). In comparison to RT7, the applicability ranges of the classical models T5 and T3 are decisively more restricted. If an error of about 5% is allowed the Mindlin–Reissner type theory can be employed for $a/h \geqslant 25$ and the Kirchhoff–Love type theory only for $a/h \geqslant 50$ while the refined model is in this sense applicable up to the value $a/h = 10$. From the numerical results presented in Table 5 one may furthermore deduce that the different types of kinematic models influence the responses for the displacement and shear stresses $s^{12}$ more than the normal stresses $s^{11}$.

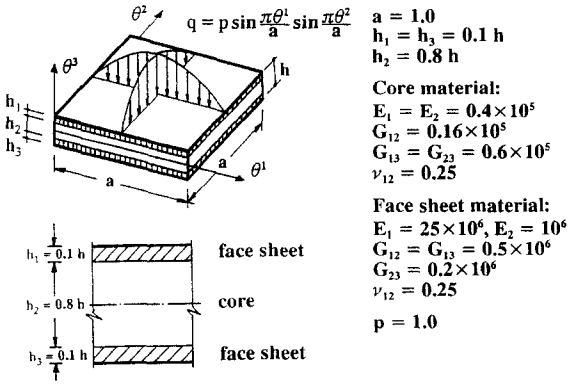


Fig. 6. Sandwich plate under sinusoidal transverse loads.

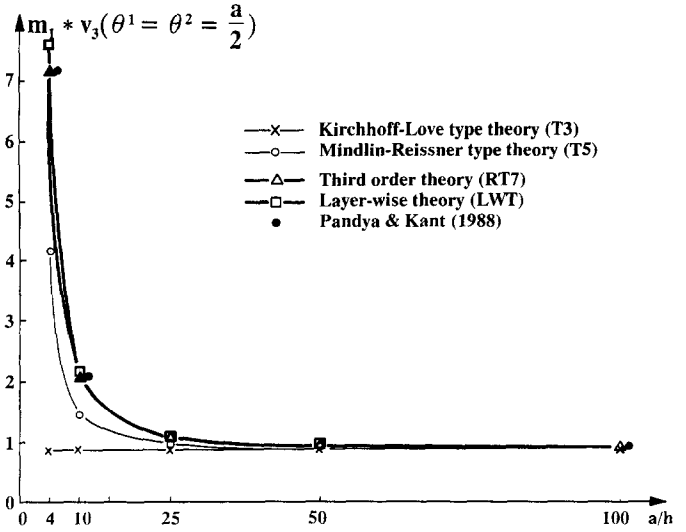


Fig. 7. Influence of the side-length to thickness ratio $a/h$ on the displacement.

*Example 2: Sandwich plate under uniform transverse load (Srinivas and Rao, 1970).* The present structure (Fig. 9) is also simply supported and consists of three layers placed symmetrically with respect to the middle surface. In contrast to the previous example the side-length to thickness ratio has been appointed, in this case as a constant value $a/h = 10$ so that the structure belongs obviously to the thick case. To show the influence of the analysis models on the responses a parameter study has been carried out by varying the modular ratio $R$, which represents the ratio of the material properties $(E, G)$ of the face sheets to those of the core. For nondimensionalizing of the results the following multipliers are used:

$$m_4 = \frac{1}{q}, \quad m_5 = \frac{C_{11}(\text{Core})}{hq}.$$

By means of the parameter $R$ layer material discontinuities can be increased arbitrarily. Now the question is what may happen in such situations?

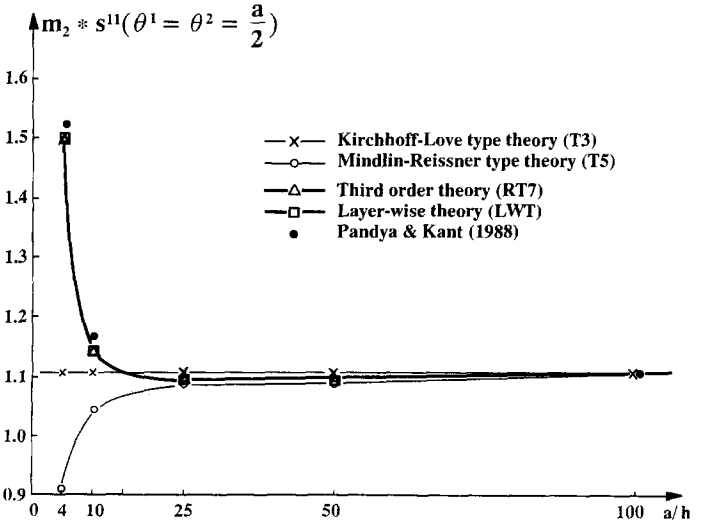


Fig. 8. Influence of the side-length to thickness ratio $a/h$ on the stresses.

Table 5. Sandwich plate under sinusoidal transverse loads—systematic comparison of different theoretical models

| Comparison of different theories: $a/h = 100.0$ | | | | | | |
|---|---|---|---|---|---|---|
| Model | $m_1 * v_{3\max}$ | $m_2 * s^{11}\left(\frac{h}{2}\right)$ | $m_2 * s^{22}\left(\frac{h}{2}\right)$ | $m_2 * s^{11}\left(\frac{4h}{10}\right)$ | $m_2 * s^{22}\left(\frac{4h}{10}\right)$ | $m_2 * s^{12}\left(\frac{h}{2}\right)$ |
| T3 | 0.8782 | 1.1060 | 0.0548 | 0.8848 | 0.0438 | −0.0433 |
| T5 | 0.8841 | 1.0916 | 0.0543 | 0.8733 | 0.0434 | −0.0433 |
| RT7 | 0.8903 | 1.0931 | 0.0547 | 0.8719 | 0.0437 | −0.0435 |
| LWT | 0.8917 | 1.0931 | 0.0547 | 0.8713 | 0.0437 | −0.0435 |
| Pandya and Kant (1988) | 0.8910 | 1.1090 | 0.0550 | 0.8847 | | −0.0437 |
| Pagano (1970) | | 1.098 | 0.0550 | 0.875 | | −0.0437 |

| Comparison of different theories: $a/h = 50.0$ | | | | | | |
|---|---|---|---|---|---|---|
| Model | $m_1 * v_{3\max}$ | $m_2 * s^{11}\left(\frac{h}{2}\right)$ | $m_2 * s^{22}\left(\frac{h}{2}\right)$ | $m_2 * s^{11}\left(\frac{4h}{10}\right)$ | $m_2 * s^{22}\left(\frac{4h}{10}\right)$ | $m_2 * s^{12}\left(\frac{h}{2}\right)$ |
| T3 | 0.8782 | 1.1060 | 0.0548 | 0.8848 | 0.0438 | −0.0433 |
| T5 | 0.9016 | 1.0874 | 0.0548 | 0.8700 | 0.0439 | −0.0435 |
| RT7 | 0.9288 | 1.0945 | 0.0564 | 0.8652 | 0.0450 | −0.0443 |
| LWT | 0.9344 | 1.0947 | 0.0566 | 0.8631 | 0.0450 | −0.0443 |

| Comparison of different theories: $a/h = 25.0$ | | | | | | |
|---|---|---|---|---|---|---|
| Model | $m_1 * v_{3\max}$ | $m_2 * s^{11}\left(\frac{h}{2}\right)$ | $m_2 * s^{22}\left(\frac{h}{2}\right)$ | $m_2 * s^{11}\left(\frac{4h}{10}\right)$ | $m_2 * s^{22}\left(\frac{4h}{10}\right)$ | $m_2 * s^{12}\left(\frac{h}{2}\right)$ |
| T3 | 0.8782 | 1.1060 | 0.0548 | 0.8848 | 0.0438 | −0.0433 |
| T5 | 0.9715 | 1.0819 | 0.0576 | 0.8655 | 0.0461 | −0.0447 |
| RT7 | 1.0816 | 1.1003 | 0.0631 | 0.8391 | 0.0499 | −0.0477 |
| LWT | 1.1027 | 1.1008 | 0.0641 | 0.8305 | 0.0506 | −0.0482 |

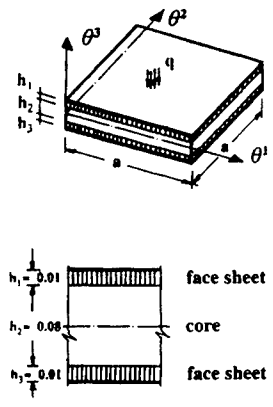


**a = 1.0**
**$h_1 = h_3 = 0.01$ , $h_2 = 0.08$**

**Core material:**

$C_{11} = E_1/(1-\nu_{12}\nu_{21})$
$= 0.999781$
$C_{12} = \nu_{12}E_2/(1-\nu_{12}\nu_{21})$
$= C_{21} = 0.231192$
$C_{22} = E_2/(1-\nu_{12}\nu_{21})$
$= 0.524886$
$C_{33} = G_{12} = 0.262931$
$C_{44} = G_{23} = 0.266810$
$C_{55} = G_{13} = 0.159914$

**Face sheet material:**

**Material constants (E, G) are obtained from those of the core material by multiplying with the modular ratio R.**

**q = 1.0**

Fig. 9. Sandwich plate under uniform transverse load.

The numerical results illustrated in Fig. 10 for the deflection $v_{3\max}(\theta^1, \theta^2 = a/2)$ and in Figs 11–12 for the stresses $s^{\alpha\alpha}_{\max}(\theta^1, \theta^2 = a/2, \theta^3 = h/2)$ show discrepancies becoming increasingly significant as the parameter $R$ increases. This is particularly the case if the results due to the refined models LWT and RT7 are compared with those due to the classical models T5 and T3. The applicability range of different models concerning the prediction of the displacement $v_3$ can be seen more clearly by examining the errors plotted in Fig. 13. We note that for the calculation of errors the values due to the layer-wise theory have been considered as reference values. In this context we emphasize the excellent agreement of the results of the layer-wise model with the 3D analytical solution given by Srinivas and Rao (1970) for the values $R = 5, 10, 15$. This fact can also be confirmed by examining numerical results presented in Table 6.

Figure 14 illustrates the distributions of transverse shear stresses $s^{13}$ across the thickness for $R = 10$, computed by different analysis models. The results presented refer to the centre point of the element near the plate corner. The piecewise constant distribution due to the layer-wise model has been replaced in Fig. 14 by a piecewise smooth curve passing through the middle surface values of the sub-elements. It is remarkable that the curve so obtained vanishes on the laminate faces, passes through the exact values due to Srinivas and Rao (1970) and, more importantly, contains no discontinuities on interfaces. The aspects mentioned clearly demonstrate the excellent predictive capability of the layer-wise theory in

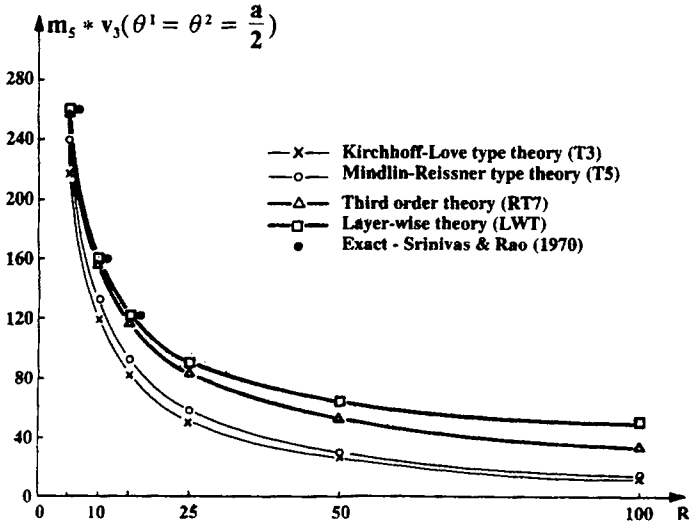


Fig. 10. Influence of the modular ratio $R$ on the displacement.

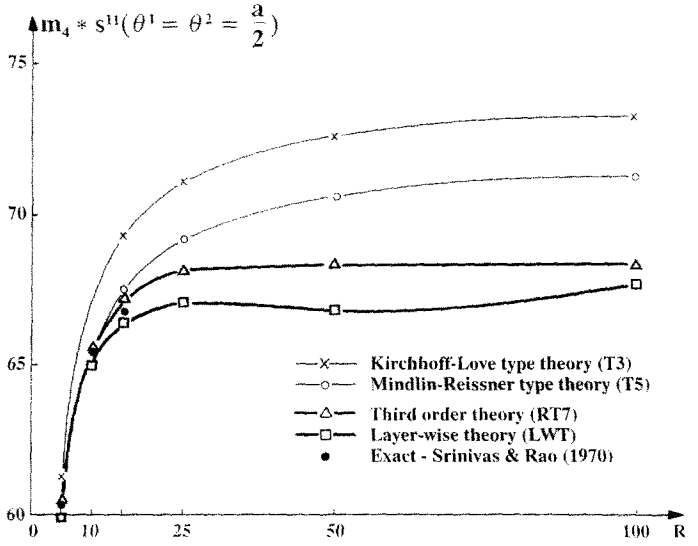


Fig. 11. Influence of the modular ratio $R$ on the stresses (I).

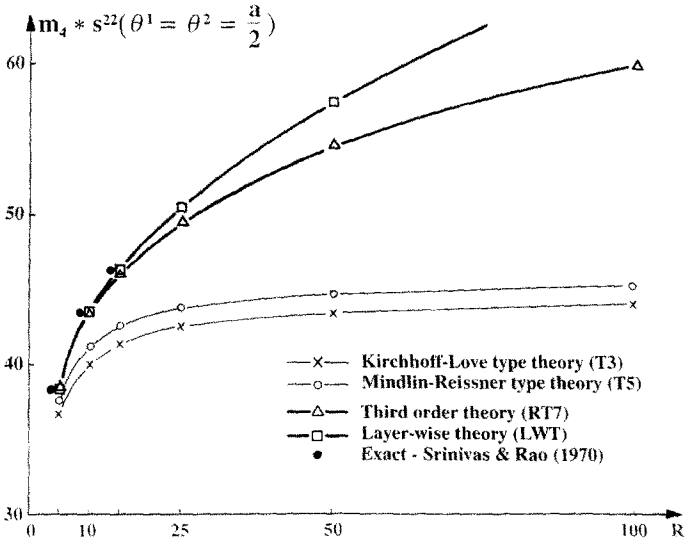


Fig. 12. Influence of the modular ratio R on the stresses (II).

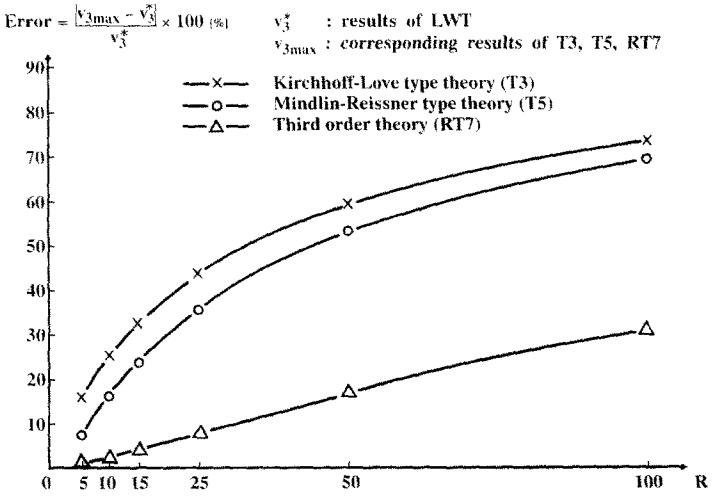


Fig. 13. Sandwich plate under uniform load—error evaluation of different theoretical models.

Table 6. Influence of the modular ratio $R$ on displacements and stresses

| | $m_5 \times v_{3\max}$ | | | | | |
|---|---|---|---|---|---|---|
| R | 5 | 10 | 15 | 25 | 50 | 100 |
| 8 × 8 T3-D4 | 216.98 | 118.79 | 81.78 | 50.39 | 25.71 | 12.99 |
| 16 × 16 T5-IAS4 | 238.81 | 132.92 | 92.20 | 57.24 | 29.39 | 14.90 |
| 16 × 16 RT7-IAS4 | 256.35 | 154.94 | 115.70 | 80.90 | 50.31 | 30.78 |
| 16 × 16 LWT-IAS4 | 259.05 | 159.50 | 121.84 | 89.66 | 63.83 | 49.77 |
| Srinivas and Rao (1970) | 258.97 | 159.38 | 121.72 | | | |
| | $m_4 \times s^{11}_{\max}$ | | | | | |
| R | 5 | 10 | 15 | 25 | 50 | 100 |
| 8 × 8 T3-D4 | 61.24 | 67.05 | 69.24 | 71.10 | 72.56 | 73.32 |
| 16 × 16 T5-IAS4 | 59.903 | 65.387 | 67.417 | 69.137 | 70.470 | 71.152 |
| 16 × 16 RT7-IAS4 | 60.336 | 65.480 | 67.111 | 68.117 | 68.400 | 68.542 |
| 16 × 16 LWT-IAS4 | 60.161 | 65.115 | 66.556 | 67.200 | 66.956 | 67.859 |
| Srinivas and Rao (1970) | 60.353 | 65.332 | 66.787 | | | |
| | $m_4 \times s^{22}_{\max}$ | | | | | |
| R | 5 | 10 | 15 | 25 | 50 | 100 |
| 8 × 8 T3-D4 | 36.66 | 40.14 | 41.45 | 42.57 | 43.44 | 43.89 |
| 16 × 16 T5-IAS4 | 37.320 | 41.009 | 42.426 | 43.629 | 44.589 | 45.087 |
| 16 × 16 RT7-IAS4 | 38.426 | 43.368 | 45.989 | 49.351 | 54.388 | 59.834 |
| 16 × 16 LWT-IAS4 | 38.450 | 43.590 | 46.481 | 50.518 | 57.596 | 67.475 |
| Srinivas and Rao (1970) | 38.491 | 43.566 | 46.424 | | | |

through-thickness modelling of shear stresses. This capability is probably due to the consideration of supplementary degrees of freedom in the layer-wise model which provides an *a priori* satisfaction of interlaminar equilibrium conditions. On the contrary, distributions calculated for $s^{13}$ by single-layer models involve large interlaminar discontinuities. But it is remarkable that the maximum value computed by the refined model RT7 has an error of only 8%. Figure 14 demonstrates the LWT model to be the best one in prediction of transverse shear stresses. A further remarkable result is that all theoretical models have led for normal stresses $s^{11}$ to nearly the same results as illustrated in Fig. 15 by a single curve. As already observed in the previous example the normal stresses $s^{\alpha\alpha}$ have also been shown in the present case to be less sensitive to the kinematic models than the displacements and particularly the shear stresses.

*Nonlinear examples*

The following nonlinear examples are presented to demonstrate that all the analysis models proposed are able to deal with nonlinear situations, involving particularly very large (finite) rotations.

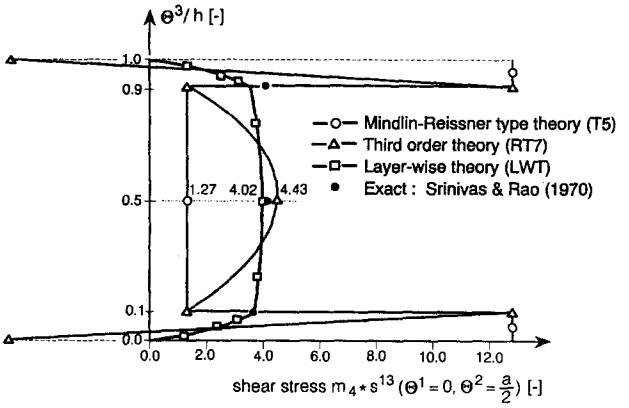


Fig. 14. Distribution of transverse shear stresses $s^{13}$ across the thickness.

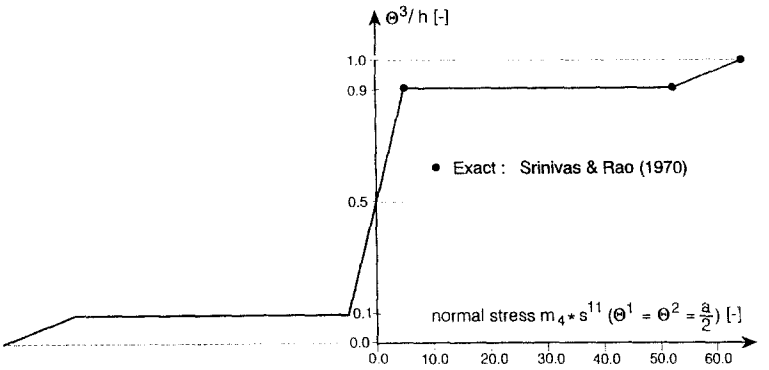


Fig. 15. Distribution of in-plane normal stresses $s^{11}$ across the thickness.

*Example 3: Cylindrical bending of an asymmetric cross-plied laminate under uniformly distributed transverse load (Reddy, 1989).* The consideration of geometrical nonlinear effects may influence the numerical results very strongly, for certain boundary conditions even at small load levels. To show this, the structure of Fig. 16 with an asymmetric lamination scheme has been analysed by the refined model RT7-IAS4 for two different boundary conditions. Numerical results obtained for the nondimensionalized maximum deflection $|v_{3\max}|/h$ by a $32 \times 1$ mesh per quarter of the structure are given in Fig. 17 and Table 7 including results due to Reddy (1989) for a systematic comparison. For pinned edges our results are for both loading cases $\pm q$ in excellent agreement with those of Reddy (1989). We note that in this case the deflection $v_3$ amounts to only four times the thickness and is accordingly of an order of magnitude as is allowed within the frame of the Donnell–Marguerre type theory being the simplest nonlinear formulation. For hinged edges allowing large displacements significant discrepancies can be observed even at small load levels. This is certainly due to the fact that in Reddy's model nonlinearities are—in contrast to the present one RT7-IAS4—not considered exactly. Discrepancies occurring in the case of the hinged edges even for small displacements clearly demonstrate the importance of the finite-rotation models concerning a reliable consideration of nonlinearities. The shear stress distribution $s^{13}$ calculated for the present asymmetric structure by the layer-wise model LWT-IAS4 (Fig. 18) is again of an excellent predictive capability. The vanishing values at $X^3 = \pm h/2$, particularly the $C^0$-continuity at the interface $X^3 = 0$, demonstrate that the corresponding equilibrium conditions are satisfied by the layer-wise model very accurately. The curves plotted in Fig. 18 have been evaluated for the linear case by a $32 \times 1$ mesh and refer to the centre point of the finite element near the support. The curve due to the layer-wise model has been obtained by a procedure similar to that used for the $s^{13}$-curve in Fig.

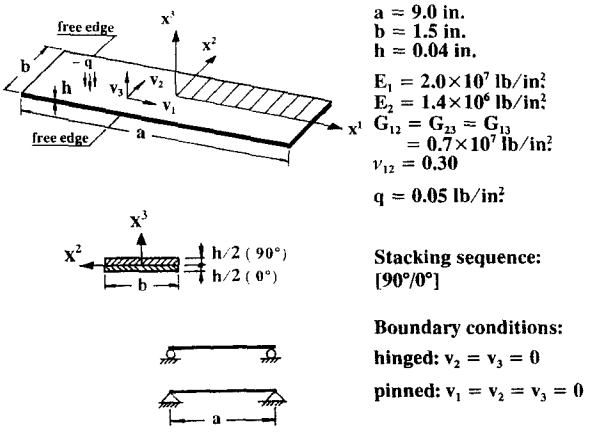


Fig. 16. Asymmetric cross-plied laminate under uniform transverse load.

Table 7. Asymmetric cross-plied laminate—nonlinear cylindrical bending

| | Pinned, $\bar{v}_{3\max} = v_{3\max}/h$ | | | | Hinged, $\bar{v}_{3\max}$ | |
|---|---|---|---|---|---|---|
| | $-q$ | | $+q$ | | $+q$ | |
| Load $q$ | Reddy (1989) | $32 \times 1$ RT7-IAS4 | Reddy (1989) | $32 \times 1$ RT7-IAS4 | Reddy (1989) | $32 \times 1$ RT7-IAS4 |
| 0.005 | −0.159 | −0.1593 | 0.475 | 0.4765 | 0.429 | 0.429 |
| 0.01 | −0.255 | −0.2553 | 0.673 | 0.6742 | 0.858 | 0.858 |
| 0.02 | −0.386 | −0.3855 | 0.847 | 0.8481 | 1.71 | 1.717 |
| 0.03 | −0.480 | −0.4790 | 0.954 | 0.9545 | 2.55 | 2.574 |
| 0.04 | −0.555 | −0.5538 | 1.034 | 1.0345 | 3.37 | 3.430 |
| 0.05 | −0.618 | −0.6169 | 1.100 | 1.1001 | 4.19 | 4.285 |
| 0.10 | −0.845 | −0.8440 | 1.327 | 1.3281 | 7.92 | 8.525 |
| 0.25 | −1.233 | −1.2301 | 1.705 | 1.7076 | 16.17 | 20.57 |
| 0.50 | −1.609 | −1.6046 | 2.075 | 2.0767 | 24.82 | 37.03 |
| 0.75 | −1.870 | −1.8649 | 2.332 | 2.3348 | 30.87 | 48.83 |
| 1.0 | −2.078 | −2.0711 | 2.532 | 2.5400 | 35.69 | 57.14 |
| 2.0 | −2.665 | −2.6543 | 3.117 | 3.1240 | 49.56 | 73.64 |
| 3.0 | −3.075 | −3.0618 | 3.525 | 3.5340 | 59.65 | 80.36 |
| 4.0 | −3.402 | −3.3853 | 3.850 | 3.8605 | 68.00 | 84.03 |
| 5.0 | −3.675 | −3.6583 | 4.125 | 4.1365 | 75.33 | 86.41 |

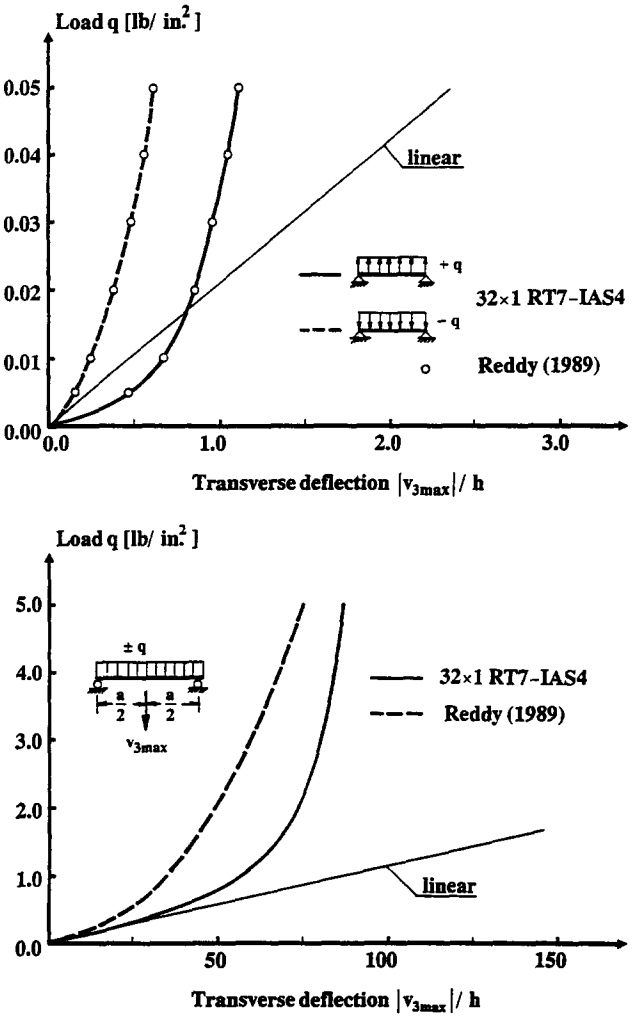


Fig. 17. Asymmetric cross-plied laminate—load–displacement diagrams.

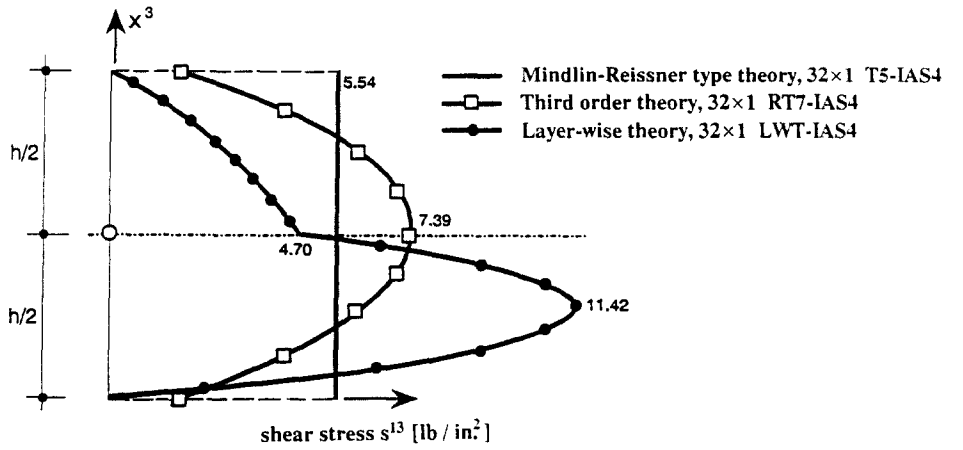


Fig. 18. Asymmetric cross-plied laminate—transverse shear stress distribution.

13. Its calculation has been achieved by 16 sub-elements across the thickness. But we note that the maximum value $s^{13}_{\max} = 9.49$ lb in$^{-2}$ calculated by this model with only 4 sub-elements can be seen as satisfactory and demonstrates the remarkable accuracy of this model. From Fig. 18 it can also be seen that, concerning a quantitative prediction of $s^{13}_{\max}$, the refined model RT7 does not show the same performance as in the previous symmetrical structure (Fig. 13). This is caused by the basic assumption of this model, the symmetrical distribution of transverse shear strains, which evidently does not hold for the present asymmetric structure. Because of this fact results due to RT7-IAS4 are, in the present case, not decisively superior to those obtained by the Mindlin–Reissner type model. We finally emphasise the very good agreement of the numerical results for the normal stresses $s^{xx}$.

*Example 4: Hyperboloidal shell under two pairs of opposite point loads.* This example (Fig. 19) finally has to demonstrate the applicability of the analysis models to arbitrary shell geometries and very strong nonlinearities. The structure consists of three layers placed symmetrically with respect to the middle surface. Due to the existing symmetries only one octant of the structure has been analysed with a $28 \times 28$ mesh by the models T5-IAS4 and RT7-IAS4. The analysis has been carried out for two different stacking sequences [0°/90°/0°] and [90°/0°/90°]. The corresponding results illustrated in Fig. 20 for the displacements $\Delta X^x$ of the characteristic points $A$, $B$, $C$ and $D$, particularly 3D-plots of Fig. 21 demonstrate the considerable influence of the lamination arrangement on the deformation behaviour. Since the main bending action occurs in the circumferential direction the structure behaves

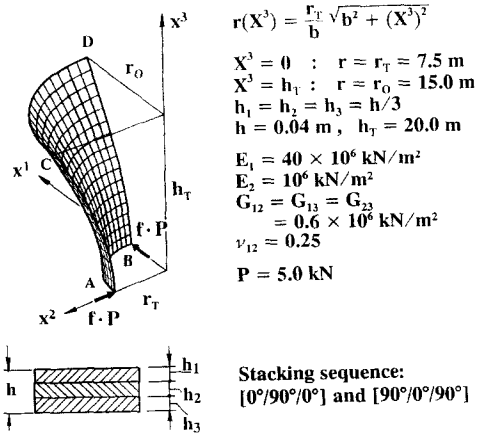


Fig. 19. Hyperboloidal shell under two pairs of opposite point loads.

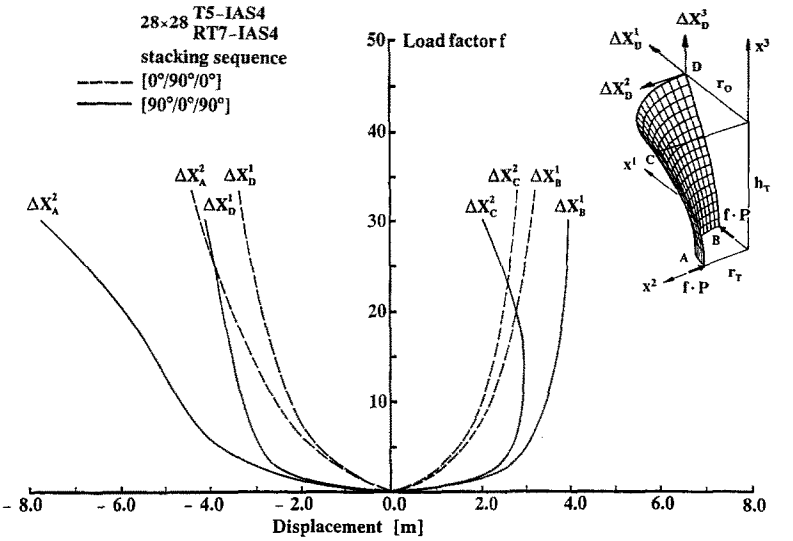


Fig. 20. Hyperboloidal shell—load–displacement diagrams.

decisively more stiffly if the face sheets ([0°/90°/0°]) but not the core ([90°/0°/90°]) are reinforced in the circumferential direction. The deformed configurations presented in Fig. 21 for the load level $f = 32.0$ demonstrate, in addition, the very large rotations and displacements involved in this example. In this context it is interesting to note that the very large deformations induced at the points $A$ and $B$ by the loads are transmitted in the same order of magnitude up to the boundary curves of the structure: An effect due to the asymptotical lines involved in the shell of negative Gaussian curvature.

## 12. CONCLUSIONS

Starting from a seven-parametric third-order theory, five theoretical models of different accuracy levels have been derived for the finite-rotation analysis of arbitrary multilayered shell structures. Special care has been taken for the definition of internal forces being geometrically interpretable on the deformed shell element.

With the exception of the five-parametric third-order theory all other models have been transformed into adequate finite element models, using in the case of shear-deformation

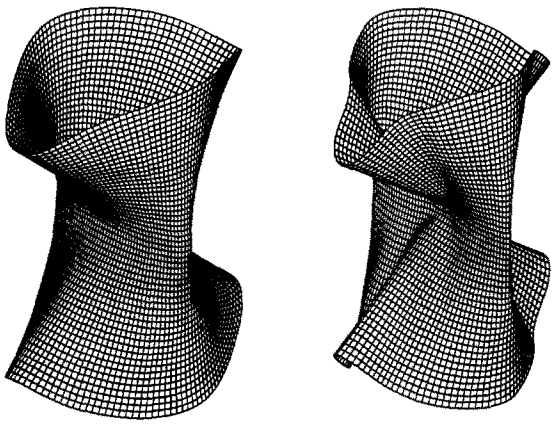

**stacking sequence [0°/90°/0°]** **stacking sequence [90°/0°/90°]**

Fig. 21. Hyperboloidal shell—deformed configurations for the load level $f = 32.0$.

models the assumed strain concept (Dvorkin and Bathe, 1984) as remedy against shear-locking. The Mindlin–Reissner type theory has also been transformed into hybrid-mixed models described in detail for the isotropic case in Ding (1989) and Başar *et al.* (1992a).

By means of extended numerical studies the following conclusions can be made about the efficiency of the theoretical models developed. The Kirchhoff–Love type theory T3 is applicable to very thin structures and not predictive in the calculation of shear deformations. Thus, its application to laminates presents no special advantages. In this sense the Mindlin–Reissner type theory T5 is much more predictive. It may provide an accurate analysis if the shell thickness and interlaminar stiffness discontinuities do not exceed certain limits depending strongly upon the application field. A decision about the applicability of this model may be made by means of the refined models RT7 and LWT. Concerning the above cited aspects the third-order theory RT7 possesses a decisively larger range of applicability. This model is not necessarily superior to the previous one T5 in prediction of the qualitative distribution of transverse shear stresses but in many cases more accurate in calculation of the corresponding maximum values. The layer-wise theory is the most predictive one and able to simulate even 3D structures with a remarkable accuracy. Its application is particularly recommended for those situations where a very accurate through-thickness modelling is primarily required.

The theoretical model RT5 is, concerning the number of independent displacements, less expensive than the model RT7, but requires in the numerical implementation higher order interpolations to achieve the same accuracy order. This is due to the second order derivatives of the displacements $v_i$, which occur because of the constraint (34) in the kinematic relations associated with the third-order strain $\overset{3}{\gamma}_{\alpha\beta}$. Concerning the numerical implementation the model RT5 therefore is comparable with the Kirchhoff–Love type theory and thus less attractive than RT7.

The finite shell elements RT7-IAS4 and LWT-IAS4 developed by means of the refined theoretical models are locking-free and applicable to strongly nonlinear situations without any numerical difficulties. They are also, like the element T5-IAS4, highly insensitive to element distortions. This is due to the isoparametric concept used in the development. In one example rectangular elements have been distorted into triangular ones and the errors induced were less than 3% (Montag, 1992). The numerical efficiency of other finite element models on the basis of classical theories has been demonstrated in earlier presentations (Başar and Ding, 1990; Başar *et al.*, 1991).

Evidently, the finite element models based on the higher-order theory and the layer-wise theory are more expensive than those based on the Mindlin–Reissner type theory. For the linear analysis of a semispherical shell under concentrated forces as given in Başar *et al.* (1991), the element RT7-IAS4 requires about twice as much as the CPU time needed by the element T5-IAS4 under the same discretization. The computational efforts required by the element LWT-IAS4 are dependent on the desired accuracy of the shear stress distribution and thereby on the number of subdivisions across the thickness.

The above discussion indicates that a single model can hardly be seen as the best one for all purposes. In reality, a decision about the quality of an analysis model can be made under consideration of the requirements of the application field. In this sense we are of the opinion that the models proposed here would enable us to select the best possible one for each individual laminate problem.

*Acknowledgement*—The present study is supported by a research grant from the German National Science Foundation (DFG) under Ba 969/2-1. This support is gratefully acknowledged.

## REFERENCES

Başar, Y. (1987). A consistent theory of geometrically non-linear shells with an independent rotation vector. *Int. J. Solids Structures* **23,** 1401–1445.

Başar, Y. (1993). Finite-rotation theories for arbitrary composite laminates. *Acta Mech.* **98,** 159–176.

Başar, Y. and Ding, Y. (1990). Finite-rotation elements for the nonlinear analysis of thin shell structures, *Int. J. Solids Structures* **26,** 83–97.

Başar, Y., Ding, Y. and Krätzig, W. B. (1992a). Finite-rotation shell elements via mixed formulation. *Comput. Mech.* **10,** 289–306.

Başar, Y., Ding, Y. and Schultz, R. (1991). Finite-elements for finite-rotation and stability analysis of composite shell structures. *International Colloquium Buckling of Shell Structures, on Land, in the Sea and in the Air*, pp. 429–437, 17–19 September 1991, Lyon, France. Elsevier Applied Science, London.

Başar, Y., Ding, Y., Schultz, R. and Montag, U. (1992b). Shear-deformation models for the finite-rotation analysis of multilayered shell structures. *Modelling of Shells with Nonlinear Behaviour, EUROMECH Colloquium 292*, 2–4 September 1992, Munich, Germany.

Başar, Y. and Krätzig, W. B. (1985). *Mechanik der Flächentragwerke*. Friedr. Vieweg und Sohn, Braunschweig/Wiesbaden.

Başar, Y. and Krätzig, W. B. (1990). Introduction into finite-rotation shell theories and their operator formulation. In *Computational Mechanics of Nonlinear Response of Shells* (Edited by W. B. Krätzig and E. Onate). Springer, Berlin.

Bicos, A. S. and Springer, G. S. (1989). Analysis of free damped vibration of laminated composite plates and shells. *Int. J. Solids Structures* **25,** 129–149.

Büchter, N. (1992). Zusammenführung von Degenerationskonzept und Schalentheorie bei endlichen Deformationen. Ph.D. thesis, Universität Stuttgart, Germany.

Büchter, N. and Ramm, E. (1992). Shell theory versus degeneration—a comparison in large rotation finite element analysis. *Int. J. Num. Meth. Engng* **34,** 39–59.

Cederbaum, G. and Librescu, L. (1989). Remarks on a dynamical higher-order theory of laminated plates and its application in random vibration response. *Int. J. Solids Structures* **25,** 515–526.

Ding, Y. (1989). Finite-Rotations-Elemente zur geometrisch nichtlinearen Analyse allgemeiner Flächentragwerke. Ph.D. thesis, Institut für Statik und Dynamik, Ruhr-Universität Bochum, Germany.

Dorninger, K. (1989). Entwicklung von nichtlinearen FE-Algorithmen zur Berechnung von Schalenkonstruktionen aus Faserverbundstoffen, VDI-Fortschritt-Berichte, Reihe 18, Nr. 65, VDI Verlag, Düsseldorf, Germany.

Dorninger, K. and Rammerstorfer, F. G. (1990). A layered composite shell element for elastic and thermoelastic stress and stability analysis at large deformations. *Int. J. Num. Meth. Engng* **30,** 833–858.

Doxsee, L. E. (1989). A higher-order theory of hygrothermal behavior of laminated composite shells. *Int. J. Solids Structures* **25,** 339–355.

Dvorkin, E. N. and Bathe, K.-J. (1984). A continuum mechanics based four-node shell element for general nonlinear analysis. *Engng Comput.* **1,** 77–88.

Epstein, M. and Glocker, P. G. (1977). Nonlinear analysis of multilayered shells. *Int. J. Solids Structures* **13,** 1081–1089.

Epstein, M. and Huttelmeier, H.-P. (1983). A finite element formulation for multilayered and thick plates. *Comput. Struct.* **16,** 645–650.

Eschenauer, H. and Fuchs, W. (1987). Modelling, structural analysis, and optimization of composite structures. *Z. Flugwiss. Weltraumforsch.* **11,** 201–210.

Green, A. E. and Zerna, W. (1968). *Theoretical Elasticity*, 2. Auflage, at the Clarendon Press, Oxford.

Gruttmann, F., Stein, E. and Wriggers, P. (1989). Theory and numerics of thin elastic shells with finite rotations. *Ing. Archiv.* **59,** 54–67.

Klarmann, R. (1991). Nichtlineare Finite Element Berechnungen von Schalentragwerken mit geschichtetem anisotropen Querschnitt. Institut für Baustatik, Universität Friedericana Karlsruhe (TH), Schriftenreihe Heft 12, Karlsruhe 1991.

Kwon, Y. W. and Akin, J. E. (1987). Analysis of layered composite plates using a high-order deformation theory. *Comput. Struct.* **27,** 619–623.

Lo, K. H., Christensen, R. M. and Wu, E. M. (1977). A higher-order theory of plate deformation, part 2: laminated plates. *J. Appl. Mech. ASME* **44,** 663–676.

Montag, U. (1992). Die Entwicklung eines isoparametrischen Finite-Element Berechnungsmodelles für die nichtlineare Analyse faserverstärkter Laminate. Master thesis, Institut für Statik und Dynamik, Ruhr-Universität Bochum, January 1992.

Nolte, L.-P. (1983). Beitrag zur Herleitung und vergleichende Untersuchung geometrisch nichtlinearer Schalentheorien unter Berücksichtigung großer Rotationen. Mitteilung aus dem Institut für Mechanik, Nr. 39, Dez. 1983, Ruhr-Universität Bochum, Germany.

Noor, A. K., Burton, W. S. and Peters, J. M. (1991). Assessment of computational models for multilayered composite cylinders. *Int. J. Solids Structures* **27,** 1269–1286.

Owen, D. R. J. and Li, Z. H. (1987a). A refined analysis of laminated plates by finite element displacement methods—I. Fundamentals and static analysis. *Comput. Struct.* **26,** 907–914.

Owen, D. R. J. and Li, Z. H. (1987b). A refined analysis of laminated plates by finite element displacement methods—II. Vibration and stability. *Comput. Struct.* **26,** 915–923.

Palazotto, A. N. and Linnemann, P. E. (1991). Vibration and buckling characteristics of composite cylindrical panels incorporating the effects of a higher order shear theory. *Int. J. Solids Structures* **28,** 341–361.

Palmerio, A. F., Reddy, J. N. and Schmidt, R. (1990a). On a moderate rotation theory of laminated anisotropic shells, part 1: Theory. *Int. J. Nonlin. Mech.* **25,** 687–700.

Palmerio, A. F., Reddy, J. N. and Schmidt, R. (1990b). On a moderate rotation theory of laminated anisotropic shells, part 2: Finite-element analysis. *Int. J. Nonlin. Mech.* **25,** 701–714.

Pandya, B. N. and Kant, T. (1988). Higher-order shear deformable theories for flexure of sandwich plates—finite element evaluations. *Int. J. Solids Structures* **24**(12), 1267–1286.

Phan, N. D. and Reddy, J. N. (1985). Analysis of laminated composite plates using a higher-order shear deformation theory. *Int. J. Num. Meth. Engng* **21,** 2201–2219.

Pietraszkiewicz, W. (1984). Lagrangian description and incremental formulation in the nonlinear theory of thin shells. *Int. J. Nonlin. Mech.* **19,** 115–140.

Pietraszkiewicz, W. (1989). Geometrically nonlinear theories of thin elastic shells. *Adv. Mech.* **12**(1), 52–130.

Ramm, E. (1976). Geometrisch Nichtlineare Elastostatik und Finite Elemente, Habilitationsschrift Bericht Nr. 76-2, Institut für Baustatik der Universität Stuttgart, Germany.

Rammerstorfer, F. G. (1991). CISM course "nonlinear analysis of shells by finite elements", Lectures on "composite and sandwich shells", Udine.

Recke, L. and Wunderlich, W. (1986). Rotations as primary unknowns in the nonlinear theory of shells and corresponding finite element models. In *Finite Rotations in Structural Mechanics* (Edited by W. Pietraszkiewicz), pp. 239–258. Springer, Berlin.

Reddy, J. N. (1984). A simple high-order theory for laminated composite plates. *J. Appl. Mech.* **51,** 745–752.

Reddy, J. N. (1989). On refined computational models of composite laminates. *Int. J. Num. Meth. Engng* **27,** 361–382.

Reddy, J. N., Barbero, E. J. and Teply, J. L. (1989). A plate bending element based on a generalized laminate plate theory. *Int. J. Num. Meth. Engng* **28,** 2275–2292.

Reissner, E. (1945). The effect of transverse shear deformation on the bending of elastic plates. *J. Appl. Mech.* **12,** A69–A77.

Sansour, C. and Bufler, H. (1992). An exact finite rotation shell theory, its mixed variational formulation and its finite element implementation. *Int. J. Num. Meth. Engng* **34,** 73–115.

Seide, P. and Chaudhuri, R. A. (1987). Triangular finite element for analysis of thick laminated shells. *Int. J. Num. Meth. Engng* **24,** 1563–1579.

Shalev, D. and Aboudi, J. (1991). Postbuckling analysis of viscoelastic laminated plates using higher-order theory. *Int. J. Solids Structures* **27,** 1747–1755.

Simo, J. C. and Fox, D. D. (1989). On a stress resultant geometrically exact shell model. Part I: formulation and optimal parametrization. *Comp. Meth. Appl. Mech. Engng* **72,** 267–304.

Simo, J. C., Fox, D. D. and Rifai, M. S. (1990). On a stress resultant geometrically exact shell model. Part III: computational aspects of the nonlinear theory. *Comp. Meth. Appl. Mech. Engng* **79,** 21–70.

Srinivas, S. and Rao, A. K. (1970). Bending vibration and buckling of simply supported thick orthotropic rectangular plates and laminates. *Int. J. Solids Structures* **6,** 1463–1481.

Stein, E., Berg, A. and Wagner, W. (1982). Different levels at non-linear shell theory in finite element stability analysis. In *Buckling of Shells, Proc. of a State-of-the-Art Colloquium.* Springer, Berlin.

Stein, E., Wagner, W. and Lambertz, K. H. (1984). Geometrically nonlinear theory and incremental analysis of thin shells. In *Flexible Shells, Theory and Applications* (Edited by E. L. Axelrad and F. A. Emmerling). Springer, Berlin.